MASTER INTERNSHIP REPORT

# MODELLING PILOT PITCH CONTROL

## ANALYSIS OF HUMAN-IN-THE-LOOP DYNAMICS FROM A CONTROL THEORY PERSPECTIVE

DANIËL TAN

東京大学
THE UNIVERSITY OF TOKYO

UNIVERSITEIT TWENTE.

Daniël Tan: *Modelling Pilot Pitch Control,* Analysis of human-in-the-loop dynamics from a control theory perspective , May 2014 - October 2014

SUPERVISORS:
Dr. Ir. J.O. Entzinger
Dr. Ir. R.G.K.M Aarts
Prof. Dr. S. Suzuki

LOCATION:
Tokyo

TIME FRAME:
May 2014 - October 2014

RELEASE:
February 3, 2015

AUTHOR:
Daniël Tan
Mechanical Engineering
University of Twente
d.j.tan@student.utwente.nl

# ABSTRACT

This internship report discusses aspects of pilot modelling from a system identification perspective. The assignment is within the research project on the investigation of the safety of curved approaches at The University of Tokyo. Modelling dynamics of human pilot control could provide valuable insights on the pilot's capacity and performance. The multi-dimensional human-aircraft system is complex and consists of feedback loops. It is therefore difficult to identify the entire human-in-the-loop system. Attempts have been made to capture pitch dynamics in a predictive mathematical model.

In order to acquire control data, three types of experiments have been designed: 1) a theoretical setup to test identification techniques, 2) a computer simulation augmenting pitch dynamics of a B747-400, and 3) the setup in a full flight simulator. The procedure for the experiments is similar and the pilot is asked to track the motion of the Flight Director (FD), indicated on the Primary Flight Display (PFD). The artificial FD signal is designed using system identification theory and its frequency content is well within human bandwidth. The aircraft is trimmed to a stable and level flight and all other control inputs (e.g. ailerons, rudders, thrust) apart from the elevator have been left untouched. The data from the third experiment performed by an experienced pilot in a Dornier Do-228-200 full flight simulator has been used for analysis. All models have been evaluated on model fit, complexity and calculation time.

It is shown that a linear parametric Auto Regressive with exogenous input (ARX) model is sufficient to model the closed-loop dynamics. For controller identification, the direct identification method is used. In this case, a linear ARX model only captures course control action, but lacks the capacity to predict corrective control. A non-linear ARX (NARX) neural network provides significant better results in terms of model fit, but requires a high number of parameters and is computational intensive. Furthermore, one should be cautious with providing (elevator) feedback channels to self-learning model sets (as the with the NARX) since it can yield erroneous results. Consequently, an Adaptive Neuro-Fuzzy Inference System (ANFIS) has been modelled relying on the FD input signal and actual aircraft pitch. This approach combines fuzzy logic with characteristics of neural networks and the control strategy can be interpreted conveniently due to its linguistic rules. Although the ANFIS doesn't excel in model fit due to large occasional prediction outliers, it does capture human corrective control with only 4 fuzzy rules.

It has been hypothesised that the level of experience can be evaluated by observing the closed-loop and human control models. Further research is needed to test the generality of the modelled human control dynamics.

# ACKNOWLEDGEMENTS

Many thanks to my supervisor dr. Jorg Entzinger, who made my internship at The University of Tokyo possible. Discussing the progress during weekly meetings has been very interesting and it has been a pleasure working with him. My internship in Japan has been challenging and truly inspiring and wasn't possible without his kind support. Also a warm thank you to prof. dr. Suzuki, the head of the Department of Aeronautics and Astronautics, Mr. Matsunaga for his assistance with the laboratory simulator, and to Mr. Funabiki for the experiments conducted in the JAXA simulator.

During the internship I was able to attend some flight simulator lessons. I would sincerely like to thank Ex-JAL Captain Mr. Uemura, for sharing his flight experience and giving useful insights on pilot control action.

I would like to thank the members of the Suzuki-Tsuchiya lab for the warm welcome and an unforgettable experience. Especially Shumpei Kamo, who showed me around the university and introduced me to many aspects of the Japanese lifestyle. Our research projects aligned and he has been of great help during experiments and interpreting the results.

# CONTENTS

# LIST OF FIGURES

# LIST OF TABLES

# ACRONYMS

| | |
|---|---|
| **JAXA** | The Japan Aerospace Exploration Agency |
| **RNP** | Required Navigation Performance |
| **RNP-AR** | Required Navigation Performance - Authorization Required |
| **FD** | Flight Director |
| **PFD** | Primary Flight Display |
| **AI** | Attitude Indicator |
| **AP** | Auto Pilot |
| **SISO** | Single-Input-Single-Output |
| **MIMO** | Multi-Input-Multi-Output |
| **LTI** | Linear and Time-Invariant |
| **FIR** | Finite Impulse Response |
| **PRBS** | Pseudo-Random Binary Signal |
| **PEM** | Prediction Error Method |
| **PE** | Persistent Exciting |
| **WSS** | Wide-Sense Stationary |
| **PSD** | Power Spectral Density |
| **RMSE** | Root Mean Square Error |
| **ARMA** | Auto Regressive, Moving Average |
| **ARMAX** | Auto Regressive, Moving Average, with exogenous input |
| **ARX** | Auto Regressive with exogenous input |
| **AIC** | Akaike Information Criterion |
| **ANFIS** | Adaptive Neuro-Fuzzy Inference System |
| **NN** | Neural Network |
| **NARX** | Non-linear ARX |
| **ANOVA** | Analysis of Variances |
| **MF** | Membership Functions |

# 1 INTRODUCTION

As a part of my master's programme 'Mechanical Automation and Mechatronics' at the University of Twente, I participated in a research internship at the Department of Aeronautics and Astronautics at the University of Tokyo. This report describes my work during the course of roughly four months in Japan.

First, in this chapter, the background of the current research project and the outline of my contribution will be discussed. Next, some background information is discussed into more detail in Chapter 2 and research methods and experiment results are examined in Chapter 3 and Chapter 4. Finally, conclusions are drawn in Chapter 5 and some remarks concerning the experiments and analysis techniques are treated in Chapter 6.

## 1.1 RESEARCH PROJECT OVERVIEW

This research internship is within a project on the safety of curved approaches led by dr. Entzinger from the School of Engineering at The University of Tokyo. The project is in collaboration with and funded by The Japan Aerospace Exploration Agency (JAXA).

Recent advances in navigational technology introduced the possibility to exploit more sophisticated approach procedures. The curved approach is flown under the set of procedures called Required Navigation Performance - Authorization Required (RNP-AR). It is a more complex flight procedure, which allows the aircraft to approach the runway through a curved path. Even though pilots usually rely on cockpit automation to execute such an approach operation, the pilot should be able to take over the control of the aircraft at any time. It is believed that curved approaches are more difficult than straight approaches. It is therefore interesting to investigate the effect of the curved approach procedures on the pilot's control.

Two main objectives for this research have been defined (from the year reports for JAXA):

1. To understand differences in pilots' mental models and cognitive processes between curved and straight approaches
2. To find out how best to support the pilot (through training or interfaces) in his supervision of automation and decision making.

Until date, this research resulted in reports and publications on the pilot's workload by measuring heart rate variability and eye blinks as well as calculating the time-to-crash [13, 11, 34]. However, this subject has not yet been approached such that a dynamical model of the human pilot could be obtained. Such a model could provide more complete analysis possibilities of the pilot control action and may give valuable insights on the pilot's performance and limitations.

Modelling the dynamics of human pilot behaviour has been an active topic in literature and a short overview is given in Chapter 2. Tools from disciplines such as 'system identification' and 'artificial intelligence' could be interesting to observe in this context, as addressed in [12].

## 1.2 INTERNSHIP ASSIGNMENT

During my internship I attempted to construct a predictive mathematical model of human pilot control action. Aircraft control is multidimensional and can be very complicated to capture in a single model. Therefore, simplifications have been made, resulting an analysis of pilot pitch control only (see Chapter 2 for further explanation).

In this section, a brief overview of the internship assignment will be given. The scope of my internship assignment has been shown graphically in Figure 1. It shows the progress of the assignment over time and what has been the main focus during different stages of the assignment. In short, my contribution to the research project can be described as:

- Investigating closed-loop dynamics of the human-machine (pilot-aircraft) interaction
- To determine a suitable model-set to capture human pilot pitch control action.

The first part of the internship was devoted to preparation and exploration of the field of subject. This involved reviewing available literature in the field of system identification and human (pilot) modelling. In addition to the courses 'System Identification and Parameter Estimation' and 'Time Series Analysis' at the University of Twente, the literature review functioned as fundamentals for outlining the experiments and the theory behind modelling the system's behaviour. These topics which will be discussed throughout this report.

A great part of the time was spent on designing and conducting experiments in order to retrieve pilot control data. Several analysis techniques have been used to process the data. For that purpose, several MATLAB scripts have written and are collected in the 'Pilot Identification Toolbox' which, together with this report, is one of the deliverables of the internship. The scripts in the toolbox can be executed for data acquisition and the calculation of the human pilot (pitch) control model. For further information about the toolbox and instructions for its usage, see Appendix F.

The experiment data is used to construct models of human-in-the-loop system and pilot control action. Linear and non-linear modelling techniques have been evaluated and are discussed in Chapter 4.

Only the pitch dynamics have been considered in this work and this report can be seen as a 'case study'. Future experiments can be performed in similar manner, even if the focus might not be on pitch dynamics.

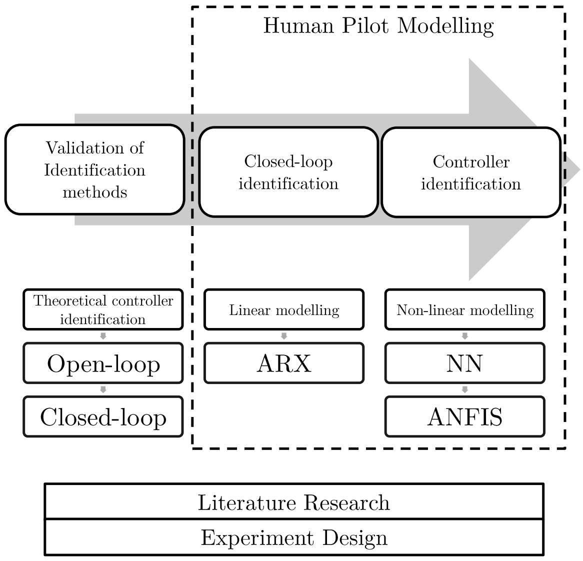
Human Pilot Modelling
Validation of Identification methods
Closed-loop identification
Controller identification
Theoretical controller identification
Open-loop
Closed-loop
Linear modelling
ARX
Non-linear modelling
NN
ANFIS
Literature Research
Experiment Design

Figure 1: A graphical overview of the internship. It can roughly be divided into three stages as indicated by the grey arrow. The analysis techniques for the control models can be found below. Experiment design and literature reviews have been performed throughout the internship.

The procedures have been outlined and possible pitfalls attempted to be addressed in a general sense. Therefore, this work could be considered as consulting report for the identification of the human pilot dynamics.

# 2 BACKGROUND INFORMATION

This chapter provides the reader some background information. Essential information about flight dynamics and aircraft control are given in Section 2.1. Section 2.2 elaborates on prerequisite simplifications and assumptions to narrow the scope of the assignment. In addition to Appendix A, Section 2.3, some basic information on human pilot modelling is treated.

## 2.1 BASIC FLIGHT DYNAMICS

Plenty of information about aircraft dynamics can be found in literature. Those works mainly cover the derivation of the equations of motion, its linearisation, and fluid dynamic properties of the wing. For these topics, the report refers to the available literature. Some aspects do need to be discussed here, such as the basic concepts of controlling an aircraft.

During flight, the aircraft is a system in 3D space which can be manipulated in three rotational axis. Rotation along the longitudinal axis is called roll, along the lateral axis pitch and along the vertical axis yaw. The axis meet in the aircraft's centre of gravity. See Figure 2 for a graphical explanation.

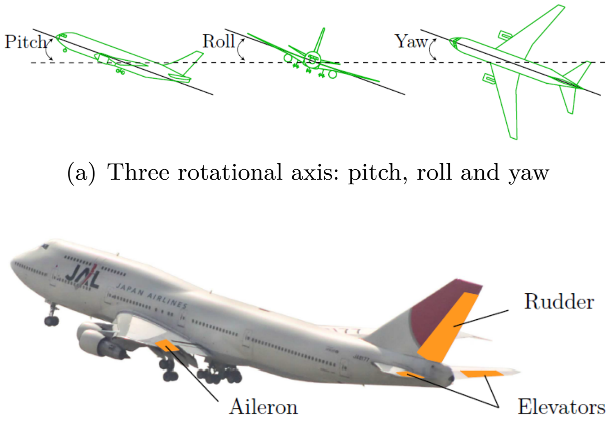

(a) Three rotational axis: pitch, roll and yaw

(b) The aircraft's primary control surfaces

Figure 2: An aircraft's primary controls. The pitch, roll and yaw can be influenced by controlling the elevator, ailerons and rudder respectively. Figure from [12].

To control an aircraft, generally control surfaces are used. These can be categorized by *primary control surfaces* and *secondary control surfaces*. The primary control surfaces are the control surfaces essential to control the aircraft, such as elevators, ailerons and rudder. Without these the aircraft will be uncontrollable. Secondary control surfaces include flaps and trim tabs and are used to tune the aircraft so that it can be controlled more conveniently. Table 1 shows which primary control surface affects which degree of freedom. Note that the control of the aircraft is not decoupled as insinuated in Table 1 and all control surfaces (indirectly) affect all degrees of freedom.

| Axis | | Control surface |
|---|---|---|
| Longitudinal | Roll | Aileron |
| Lateral | Pitch | Elevator |
| Vertical | Yaw | Rudder |

Table 1: Every control surface mainly influences one rotational degree of freedom. Note that this table is simplified: aircraft control is highly coupled and all control surfaces indirectly affect other degrees of freedom.

The aircraft can be modelled as a dynamical system with inputs and outputs. In this report, primary control surfaces will be considered as the control input, whereas the secondary control surfaces will be set to remain constant and can be considered as ‘aircraft settings’. For instance, landing gear and thrust settings influence flight dynamics but do not relate to control surfaces. The outputs are the aircraft states (e.g. the position, and velocity in 3D space) and proxies of these states, indicated on cockpit instruments.

## 2.2 SIMPLIFICATIONS AND ASSUMPTIONS

Aircraft control is a multidimensional control task. In order to illustrate simplifications in the internship assignment, matrix $C$ in Equation 1 is introduced. It maps an input vector [elevator, ailerons, rudder]$^T$ to [pitch, roll, yaw]$^T$ output[1]. The input of the control surface does not only influence the primary rotation axis and is coupled to all other rotations. Consequently, if the aircraft is modelled as in Figure 3, the non-diagonal terms of the control matrix will be non-zero which is characteristic for a Multi-Input-Multi-Output (MIMO) system:

$$C = \begin{bmatrix} c_{11} & c_{12} & \dots & c_{13} \\ c_{21} & c_{22} & \dots & c_{23} \\ c_{31} & c_{12} & \dots & c_{33} \end{bmatrix} \tag{1}$$

which describes a highly simplified aircraft control. The matrix elements $c_{ij}$ map the $i$-th input (which is a primary control surface) to the $j$-th output (a rotational axis in 3D space). For instance, $c_{ij}$ could be a transfer function.

The choice has been made to investigate the pilot’s pitch dynamics for the main reason that the longitudinal axis is the dominantly controlled rotation during flight. An adjustment in the pitch angle will

[1] This is a highly simplified way of representing aircraft control.

over time result in a change in altitude and glide-slope, which are two important factors during approach procedures. Also during a curved manoeuvre (which involves rolling motion of the aircraft), pitch control is of significant importance since the speed of the turn can be regulated. Since the main research project is on curved approach procedures, one could reason that modelling pilot pitch control is valid to start with.

For the experiments in this report it is assumed that pitch control can be isolated as an element from matrix $C$ in Equation 1. Only the elevator to pitch element will be considered. Although this does not directly imply decoupling of the control action, all other inputs than elevator inputs that influence the pitch angle will be ignored. This results in a Single-Input-Single-Output (SISO) system as depicted in Figure 3 and only describes the dynamics of the corresponding matrix element of $C$.

In practice, this can be done by disabling or ignoring all controls other than the elevator input from the flight simulator (see Chapter 3). This is clearly an artificial restraint, but ensures the recorded data only contains human control action around the lateral axis.

It is furthermore assumed that *during* experiments, the aircraft dynamics will remain constant, in sense that initial conditions such as secondary control surface settings and thrust level will be left untouched. Additionally, for simulation purposes, flight conditions will be excellent (i.e. no wind and no turbulence, clear weather), unless otherwise stated.

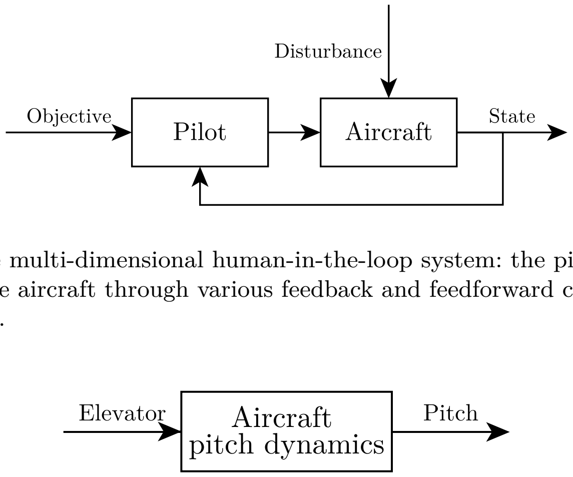

(a) The multi-dimensional human-in-the-loop system: the pilot controls the aircraft through various feedback and feedforward channels (MIMO).

(b) Highly simplified aircraft model. It only captures dynamics from elevator input to aircraft pitch output (SISO)

Figure 3: Aircraft control is a multi-dimensional problem and the internship is limited to pitch dynamics only.

## 2.3 INTRODUCTION TO HUMAN PILOT MODELLING

Modelling the control action of a human in man-machine interfacing systems can be rather complex. Human control can be considered highly non-linear and non-time-invariant as they can change control strategy any time and during operation. “[...] Consequently, two pilots may describe similar flight paths, but control the aircraft in very different manners" [12], which indicates the complexity of human control. Efforts have been made to capture parts of human control. Entzinger [12], Yilmaz et al. [55] give an overview of conventional methods, including:

- (Quasi-)linear identification
  - Cross-over model (also see [31])
  - Precision model
  - Quasi-linear model
- Optimal control and Kalman filter models
- Linear and non-linear parametric models
- Identification methods from artificial intelligence
  - Neural models
  - Fuzzy models
  - Neuro-fuzzy models
- Other models
  - Cognitive architectures (also see [35])
  - ...

In this report, linear parametric models and identification methods from artificial intelligence will be examined.

# 3 EXPERIMENT DESIGN

In the previous chapter some simplifications have been made, reducing the assignment from observing the entire aircraft control to pitch control only. See the block diagrams in Figure 3.

Essentially, a predictive mathematical model of the pilot's behaviour has to be obtained. From system identification theory it is know to be possible to capture system characteristics under certain conditions. It is always based on input- and observed output signals, but especially the input signal has to satisfy certain requirements in order to build an unbiased and consistent model. See Appendix A for a synopsis about system identification theory. Constructing a model from the collected data will be done in Chatper 4. This chapter covers the design of the experiments to capture the data from pilot dynamics.

First of all, two concepts have to be clarified that affect the pilot identification process.

## 3.1 OPEN-LOOP VS. CLOSED-LOOP

Open-loop system identification can be rather straightforward and methods are extensively described in literature (for instance, the field's leading textbooks are [28] and [45]). However, as described in Appendix A, closed-loop identification can be quite challenging, mainly due to the correlation between the reference noise inputs and outputs. Clearly, as depicted in Figure 4, the Pilot-Aircraft system can be described as a closed-loop system (when pitch control is concerned). The data should be captured and processed with care.

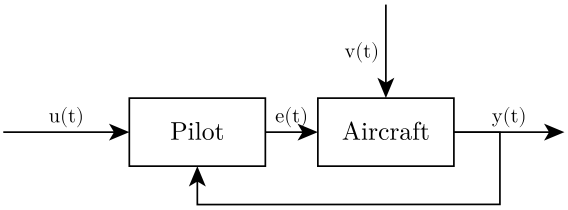

Figure 4: The closed-loop system where $u(t)$ is the pilot's pitch objective (reference input), $e(t)$ the pilot's elevator response, $v(t)$ the disturbance on the aircraft and $y(t)$ the actual aircraft pitch

## 3.2 METHODS AND MATERIALS

On first sight, the combination of possible non-linearities and the closed-loop configuration resemble a complex system to perform identification on. Therefore individual effects could be evaluated by splitting the problem up even more. Three experiments have been designed in order to gradually increase the experiment complexity. This allows to verify the effectiveness of analysis techniques. Guidelines from [28], [45] and [1] are used to design the experiments. Appendix E provides an overview of the specifications of the software and hardware used during the experiments.

### 3.2.1 *General experiment setup*

In general, the following experiments have in common that only the pitch control of the aircraft is concerned (see 'Simplifications and Assumptions' in Chapter 2). Consider the closed-loop control diagram in Figure 4.

The reference (target) input is the control objective of the pilot. It can, for instance, be a constant or varying pitch over time. Within the following experiments, this target information is displayed through the FD on the PFD which contains the Attitude Indicator (AI). Originally, the FD is an overlaid indicator on the AI that shows the required attitude of the aircraft in order to maintain a certain trajectory. The proper attitude is obtained by calculation. The FD usually consists of two perpendicular lines (crosshair configuration) and the pilot adjusts the aircraft's pitch and roll in order to align with the FD. The FD is often directly coupled to the Auto Pilot (AP), but can also be used as a stand-alone guideline for the pilot's control. This property makes it very suitable to use the FD for displaying the reference signal. In the experiments, however, the FD will not be used to guide the aircraft through a selected path, but rather to force the pilot to realize a certain pitch angle. Figure 5 shows a simplified version of the AI with FD. Note that since pitch control is considered, only the horizontal bar of the FD will be active. The pilot will be asked to follow this bar by pitching the aircraft through the cockpit's yoke. Note that it is assumed that the yoke input is proportionate with the aircraft's elevator deflection (as in Boeing-type aircrafts). In this report, 'pilot control output' is therefore also proportionate to 'elevator input'.

The output of the system in Figure 4 is the actual pitch angle of the aircraft, which is indicated on the AI and can be easily be logged. The system is influenced by perturbations such as wind and turbulence, indicated as system noise.

This approach is similar to Ertugrul [14], where a human operator is asked to track a signal on the computer screen using a mouse. The main difference with the experiments in this report is the complexity of the plant. Whereas the plant from Ertugrul [14] is just a gain, the plant in the closed-loop system in this case is a simulated aircraft.

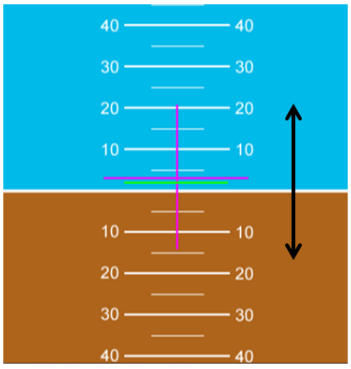

Figure 5: Graphical representation of the AI as used in the experiments described below. The green bar represents the actual aircraft pitch and will remain centred on the screen. The scale will slide underneath it. The white boundary between the blue and brown areas is the artificial horizon. The magenta FD indicates the desired attitude by moving the crosshair over the AI-scale. As only pitch dynamics are concerned, only the horizontal bar will move

### 3.2.2 *Testing closed-loop identification techniques*

Before moving on to human-in-the-loop simulations, the system identification methods have been investigated. In order to get a better understanding of this field of subject, both open-loop and closed-loop simulations have been performed *without* the presence of a human controller. Instead, a PID controller replaces the human pilot. This approach allows to bypass the potentially complex (and unknown) human control action. Figure 6 shows the block diagrams of the open- and closed-loop situation.

The aircraft model is a second order mass-spring-damper system with a crossover frequency that roughly approximates the crossover frequency of a B747 aircraft. The PID controller is designed by fixed equations so the response of the system can be simulated (and is *known* a priori). The system has been designed to be comparable with the 'actual' human-in-the-loop system but is clearly a more abstracted representation.

A second advantage is that simulation doesn't have to be performed in real-time as there is no human interaction. In Appendix B a more detailed description of this experiment setup is given, including plant and aircraft transfer functions, system noise levels and so forth. The construction of the reference input signal is described in Section 3.4.

### 3.2.3 *Computer simulation experiment*

Next, a computer simulation experiment has been designed. The human pilot has been introduced in the feedback loop (see the block diagram in Figure 7). Note that the loop is closed by the human itself and an open-loop system is non-existent in this setup. The two main features of this experiment will be pointed out.

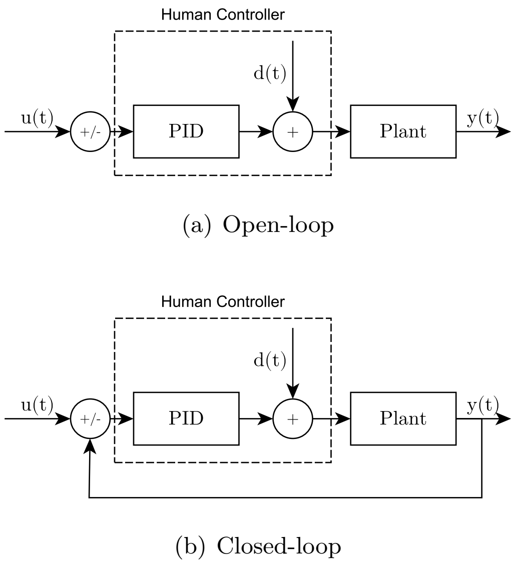

(a) Open-loop

(b) Closed-loop

Figure 6: In order to test closed-loop identification techniques, the human pilot has been replaced by a PID controller. Hence, open-loop and closed-loop simulations can be performed

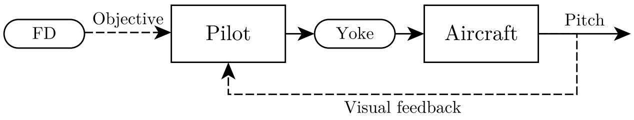

Figure 7: The experiment setup with the pilot in the loop. The pilot controls the aircraft's pitch with the yoke. The pitch is indicated on the AI. The pilot is asked to track the FD reference signal.

1. The pilot controls the pitch of the aircraft by operating the elevator with the yoke. As only pitch control is investigated, all other control inputs (e.g. roll and yaw) are ignored. Visual feedback of the aircraft's pitch is provided via a computer screen displaying a simplified version of the AI and FD[1]. A more detailed description of the software and hardware involved in this experiment can be found in Appendix E.

2. The aircraft flight dynamics are simulated in real-time. Any aircraft model could be loaded in the computer and several alternatives have been tested, such as the previously discussed second order system and models obtained from literature [25]. Additionally, attempts have been made to capture The University of Tokyo Suzuki-Tsuchiya lab B747-400 flight simulator pitch dy-

[1] The setup ensures the pilot will be fed back pitch information. However, the pitch-rate is ignored although the pilot cannot ignore this information due to the 'scrolling' representation on the AI

> namics through frequency identification techniques. The process and results are described in Appendix C.
>
> Ultimately, the model from literature has been used for simulation, for the reason that the model is defined for a greater deal of the frequency scope. It leads to a more 'realistic' feeling of an aircraft's pitch response, compared to other models. This choice is furthermore elaborated in Appendix C.

The purpose of this experiment is the same as described before. The pilot is asked to track motion of the FD by adjusting the pitch angle of the aircraft. This experiment can be performed by solely simulating the longitudinal motion of the aircraft without the need of distributing computational power to the calculation of other dynamics or graphics.

### 3.2.4 *Flight simulator experiment*

Finally, an experiment is designed for the use of JAXA's Dornier Do-228-200 full flight simulator. The pilot is now in a fully simulated environment so the full flight simulator experiment is closest to reality of the three experiment designs. The approach is the same as the computer simulation experiment: the pilot's target pitch is displayed through the FD and the pilot adjusts the aircraft pitch angle by controlling the yoke (Figure 7).

The main difference with the computer experiment, however, is that all aircraft dynamics will be calculated by the flight simulator (not only pitch movement). So influences of aileron and rudder inputs will no longer be ignored. Consequently, the pilot is given more feedback channels, which were previously eliminated by only simulating the aircraft's pitch dynamics (see the simplifications in Chapter 2). The feedback channels include visual feedback through the front window and information from many other cockpit instruments. Even though the pilot is asked to track the motion of the FD only, the pilot might not ignore the other feedback channels.

Aircraft control is a coupled system so controlling one input will not only influence the corresponding output, but will be noticeable at more system outputs. As described before, it is a MIMO system which up till now was simplified to a model that contains only elevator input to pitch output dynamics (a SISO system). With the flight simulator experiment it is formally no longer possible to reduce the human-aircraft interaction to a SISO system, but for consistency, the analysis methods will be left the same for all experiments. Still only the data from elevator to aircraft pitch will be used for analysis. When reviewing the results, the difference in experiment setup should be kept in mind.

## 3.3 PRELIMINARY TESTS

The goal of the experiments is to model the human pilot control dynamics. The structure of the experiments is described in the section above. However, there are still some parts of the experiment design that further need exploration. Some preliminary tests have to be performed for the preparation of the main experiments.

The methods used in the identification process depend on the system's behaviour. Some simple tests can provide information about various system properties for which a short description will be given. These tests have to be performed a priori and before every new experiment setup. This section contains the outline for preliminary experiments and similar tests have been carried out for the three experiment designs.

- Duration of the experiment
  The identification experiments are designed to analyse the human-machine interaction. It is interesting to know how fast the system response typically is in order to determine the minimum duration of the experiment which limits the analysis of the slowest responses of the system. From preliminary experiments, the minimum duration is determined to be in the order of 10 seconds, although generally for system identification, it is beneficial to have longer experiments in order to capture more data. Therefore, setting the maximum experiment duration is important. As human subjects are involved, there is a maximum experiment duration due to endurance, focus and workload factors. The maximum duration of the experiment is set to approximately 60 seconds[2].

- Sample frequency
  The outputs of the system are logged to a data file at a sample frequency $f_s = \frac{1}{t_s}$ [Hz] or $\omega_s = \frac{2\pi}{t_s}$ [rad/s], where $t_s$ is the sample time. For the analysis of the data in later stages, there must be enough sample points which can be achieved by making $t_s$ as small as possible.

  The upper limit of $t_s$ is set in order to still observe the highest relevant frequency, well above the Nyquist frequency [3]. Besides, there is a lower limit for $t_s$ because of the fact that *Prediction Error*-methods tend to emphasise high frequencies when $t_s$ is too small, although this problem can be resolved by re-sampling or low-pass filtering the obtained time-series a priori. More on this in [1, 28] and Appendix A

  Aarts [1] provides some rules of thumb for setting the appropriate sample frequency for a first order system with bandwidth $\omega_b$. A sample frequency such that $10\omega_b \leq \omega_s \leq 30\omega_b$ is recommended. For practical reasons, the sample times are $t_s = 0.05s$ and $t_s = 0.04s$ since this is the standard for the JAXA full flight simulator and satisfies the above criteria.

- Noise level
  McRuer [30] describes the human controller as a feedforward process with the addition of an inherent human noise input in a

[2] it could be slightly longer due to the full-length property of the PRBS, as will be discussed below

[3] Nyquist frequency $\omega_N = \frac{\omega_s}{2}$

quasi-linear pilot model. From this starting point it is useful to know the magnitude of the noise input, compared to the system's input. The amplitude of the FD pitch command for the identification experiment could be adjusted accordingly. By applying a constant reference signal to the system, the noise level can be determined by taking the square root of the variance of the fluctuating pitch output: $\sigma_v = \sqrt{var(y(t))}$. Once an estimate of $\sigma_v$ is obtained, one could achieve a suitable signal-to-noise level $\mu_{s/n}$:

$$\sigma_u = \sqrt{var(u(t))} \tag{2}$$

$$\mu_{s/n} = \frac{\sigma_v}{\sigma_u} \tag{3}$$

A signal-to-noise ratio of at least 10 is recommended for system identification experiments [1].

This is a method designed for open-loop systems. It should be kept in mind that the system is inherently closed-loop, so this test does not apply directly, but gives an indication of the noise level (and reveals control action). Another drawback is that this method will not work if the backlash of the flight simulator yoke is significant. The amplitude of the human control noise could be within the dead-zone of the yoke and will not be measurable.

- Linearity and Time invariance

  Some analysis methods require the identified system to be Linear and Time-Invariant (LTI). In short, this is due to the fact that some identification techniques require convolutions. In order to perform convolutions, the system has to be linear and time invariant.

  Let $\mathcal{H}$ be a convolution, that maps input $u$ to output $y$. This means that $y = \mathcal{H}(u)$ with $\mathcal{H} = (h * u)_n = \sum_{k=-\infty}^{\infty} h_k u_{n-k}$ and $h_1, h_2, ..., h_n \in R$ are *weights* of the system's impulse response. Note that this is a time-domain version of the more familiar transfer function. By z-transforming the input and the output of the system, the (discrete) frequency response can be found $\frac{y(e^{i\omega})}{u(e^{i\omega})} = H(e^{i\omega}) = H(z)$.

  Convolutions systems are LTI which means that:

$$\mathcal{H}(u+v) = \mathcal{H}(u) + \mathcal{H}(v) \qquad \text{additive} \tag{4}$$

$$\mathcal{H}(\alpha u) = \alpha \mathcal{H} \qquad \text{homogeneous} \tag{5}$$

$$\mathcal{H}(u_{n-k}) = \mathcal{H}(u)_{n-k} \qquad \text{time-invariant} \tag{6}$$

  The combination of homogeneity and additivity is called linearity. Gondhalekar [16] elaborates on methods to discover and characterize non-linear behaviour of a system. A straightforward method to check this property is by applying the 'staircase' signal as a reference input to the system and verifying if system's behaviour is (more or less) the same for every step. More on the background of LTI systems can be found in [26] and about preliminary tests in [1, 45, 28].

- Influence of feedback-loops
  From the assumption that the system is LTI, it is possible to preliminarily estimate it's impulse response: $y = \mathcal{H}(\delta)$, where $\delta$ is the Dirac-delta function. The Finite Impulse Response (FIR) can be calculated quite efficiently [26]. If the FIR depends only on past values of the input time series, the system is *causal*. However, it can happen that the FIR is best calculated partly with inputs of 'negative lags', which indicates output feedback. These *non-causal* FIR systems reveal the presence of one or more feedback loops, which is the case for the data acquired from the identification experiments.

## 3.4 INPUT SIGNAL GENERATION

Another important experiment design element is the composition of an appropriate reference input signal and is provided to the pilot by the FD as a pitch command. The input signal has to meet two requirements in order to provide a good basis for the identification experiment.

First of all, the signal has to be of higher amplitude than the system noise level to ensure the analysis is based on input response and not on the effects of noise. In other words, the signal to noise ratio has to be high. The most straightforward way to achieve a such, is to increase the input signal's amplitude. This, however can only be done till a certain extend due to limitations of human control.

Preliminary tests showed that human control depends on many factors and as the input signal defines the pilot's task (i.e. it is the pitch command indicated by the FD), the input also has influence on the pilot's workload (see Chapter 6). More on pilot's workload is provided by Entzinger et al. [13] and Nijenhuis [34]. When the amplitude of the reference signal is too high, it is known that pilot's tend to disengage from the experiment (The pilot will indicate that *"It is impossible to track the FD - the pitch command is too extreme and not realistic"*). This also depends on the character of the input signal (e.g. harmonic or binary) and the time the pilot has to achieve the FD position (before it changes to a new pitch command to track). In short, in order to capture pitch control dynamics, the FD has to be 'traceable' for a human pilot. The design variables for such signals are:

- Reference signal character
  Two different types of signals have been generated: a maximum-length PRBS and a periodic sum of harmonic signals (multi-sine).
- Reference signal amplitude
  The range of the FD desired pitch for the human pilot to trace
- Reference signal bandwidth
  The motion of the FD must be within the human control bandwidth

The resulting FD reference signals can be found in Figure 8 and specifications are noted in Table 2

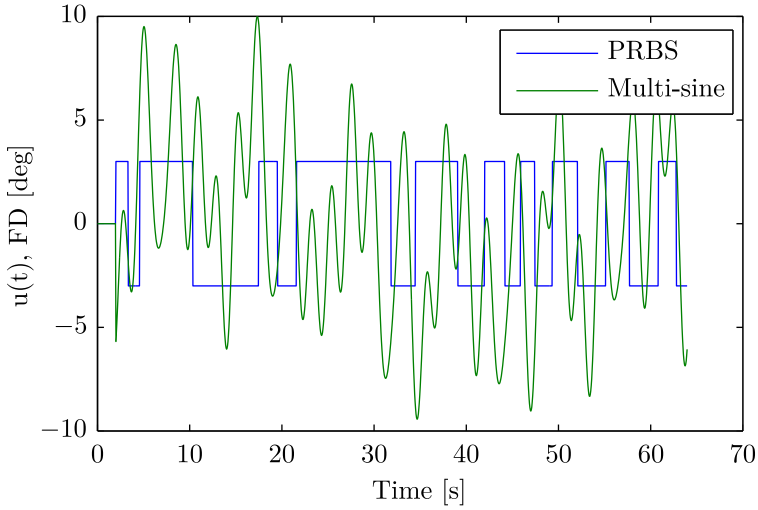

Figure 8: The FD input signals

### 3.4.1 *PRBS*

The PRBS is a periodic signal that can have two states (binary). The sequence of the states is random *within its period* and its characteristics resemble white random noise (psuedo-random). The maximum-length PRBS has a period equal to $M = 2^n - 1$ for a sequence with $n$ samples. The amplitude of the PRBS is +3 and -3 degrees around the aircraft's trimmed pitch angle and can be considered as a switching set-point reference input. The bandwidth is controlled by adjusting the clock period of the signal. The PRBS will be constant over $b$ samples resulting in a clock period of $\frac{1}{b}$. The PRBS must be traceable by the pilot. For stable operation, the normalized crossover frequency of human control is $\frac{\pi}{2}$ [31]. In order to be well within the bandwidth of human control, the PRBS is designed to have a bandwidth of 0.5 Hz.

### 3.4.2 *Multi-sine*

The multi-sine reference input is a sum of individual sines:

$$u(t) = \sum_{k=1}^{m} a_k \sin(\omega_k t + \phi_k) \tag{7}$$

where $m = 7$. The amplitudes and phases $a_k, \phi_k$ are chosen in order to obtain a smallest overall amplitude using a method proposed by Schroeder [42]. The frequency of the seven individual sine waves are again bounded in order to stay within the human bandwidth and are equally spaced in the frequency domain. Preliminary tests indicated that human pilots find it easier to trace the smooth multi-sine FD input, compared to the PRBS. Therefore, the range of the multi-sine can be larger; the desired pitch varies between -10 and 10 degrees, around the aircraft's trimmed pitch angle.

### 3.4.3 *Other input signals*

Two other FD signal types have been examined. The Dirac Delta impulse function

$$\delta(t) = \begin{cases} +\infty, & t = 0 \\ 0, & t \neq 0 \end{cases} \qquad \int_{-\infty}^{\infty} \delta(t)dt = 1 \tag{8}$$

and the Heaviside step function

$$H(t) = \begin{cases} 0, & t < 0 \\ 1, & t \geq 0 \end{cases} \qquad H(t) = \int_{-\infty}^{t} \delta(t)dt \tag{9}$$

Although these signals are convenient for their simplicity, they do not provide a good basis for identification techniques, as described in the next section.

### 3.4.4 *Persistent Excitation*

In order to estimate consistent parameters of (linear) Prediction Error Method (PEM) models, the input signal must Persistent Exciting (PE) [45]. A signal $u(t)$ is PE of order $n$ if the limit

$$R(\tau) = \lim_{N\to\infty} \frac{1}{N} \sum_{t=1}^{N} u(t+\tau)u(t) \tag{10}$$

exists and the following covariance matrix is positive definite

$$R(n) = \begin{bmatrix} R(0) & R(1) & \dots & R(n-1) \\ R(-1) & R(0) & \dots & R(n-2) \\ \vdots & \vdots & \ddots & \vdots \\ R(1-n) & R(2-n) & \dots & R(0) \end{bmatrix} \tag{11}$$

which means that

$$z^T Rz > 0 \quad \forall z \neq 0 \in \mathcal{R} \tag{12}$$

where $\tau$ is the number of lags (time shifts) of the signal. It can be shown that the order of persistent excitation reveals the frequency content of a signal and until what order the signal is uncorrelated with a delayed version of itself [45]. For example, if $u(t)$ is Gaussian distributed white noise, the signal is PE of all orders since all realisation of such 'random' process are uncorrelated. A single step input will be PE of order 1 and an impulse input is not PE for any order. In order to fit a model to the input/output data during the identification process, a high order of persistent excitation is desired. In fact, for models created by the PEM-method, the order PE($n$) limits the number of model parameters[4]. The generated input signals have been analysed on the PE property and the order $n$ is listed in Table 2. It can be seen that both the PRBS and the multi-sine signal are PE for high orders.

[4] The number of parameters $N_{param} = \frac{1}{2} n_{PE}$

| | PRBS | Multi-sine |
|---|---|---|
| Duration | 63.95 sec | 63.95 sec |
| Range | [-3,3] | [-10,10] |
| Crest factor | 1 | 2.4 |
| PE($n$) | 573 | 264 |
| Bandwidth | ± 0.5 Hz | ± 0.5 Hz |

Table 2: Properties of the input signals

### 3.4.5 *Signal properties*

Furthermore, for later processing of the time series, it is required that the reference input $u(t)$, but also the output $y(t)$ is a realization of a single (stochastic) process. $u(t)$ and $y(t)$ should be Wide-Sense Stationary (WSS) which means that the probability distribution of the input does not change over time. This results the parameters as mean and variance to be constant over time:

$$\lim_{t \to \infty} \mathbb{E}\, u(t) = \mu_u \tag{13}$$

$$\lim_{t \to \infty} \mathbb{E}\, \left( u(t) \right)^2 - \mu_u^2 = \sigma_u^2 \tag{14}$$

The signal is called ergodic if these statistical properties can be obtained by taking sufficiently long data samples of the process. Ergodicity of $u(t)$ and $y(t)$ is one of the fundamental assumptions for linear system identification so it should be considered during the conducted experiments and data acquisition.

A measure to indicate the ratio of the signal's peak values to it's average value is called the Crest factor.

$$Cr = \frac{\max |u(t)|}{u_{RMS}(t)} \tag{15}$$

$$u_{RMS} = \sqrt{\frac{1}{n}\left(u_1^2 + u_2^2 + \ldots + u_n^2\right)} \tag{16}$$

For the identification of the closed-loop system it is convenient to have input signals that have low Crest factors because they employ the amplitude range more efficiently. Binary signals have that property. However, from preliminary experiments, it is found that human pilots find it harder and more unrealistic to track a binary signal. Table 2 lists the Crest factors of the generated input signals.

### 3.4.6 *Power Spectral Density*

The frequency content of the signal can be verified by computing the PSD. Both the PSD's for the PRBS and the multi-sine have been calculated and are depicted in Figure 9 and 10. Note that the red line is the smoothed version of the 'raw' frequency domain data (the magnitude of the Fourier transform) obtained windowing the data with Welch's method [46]. Both signals primarily consist of low frequency content and are well within the human bandwidth. The multi-sine has a more or less flat power distribution in that range due to the peaks of each single sine-wave contribution. The PRBS still contains some high frequencies, because of its square-wave characteristics. In Table 2 the bandwidths of the signals have been shown. The bandwidth is defined as the frequency $\omega_{BW}$ for which the PSD drops below the $-3dB$ of its maximum value. It can be understood as the frequency interval where the majority of the signal's power is located. Preferably for system identification, one would like $\omega_{BW}$ to be as high as possible, since all frequencies will be present in the signal (white noise has this property because of its flat PSD). As described above, the human controller will then not be able to track the input, so the main frequency content should be within the human bandwidth.

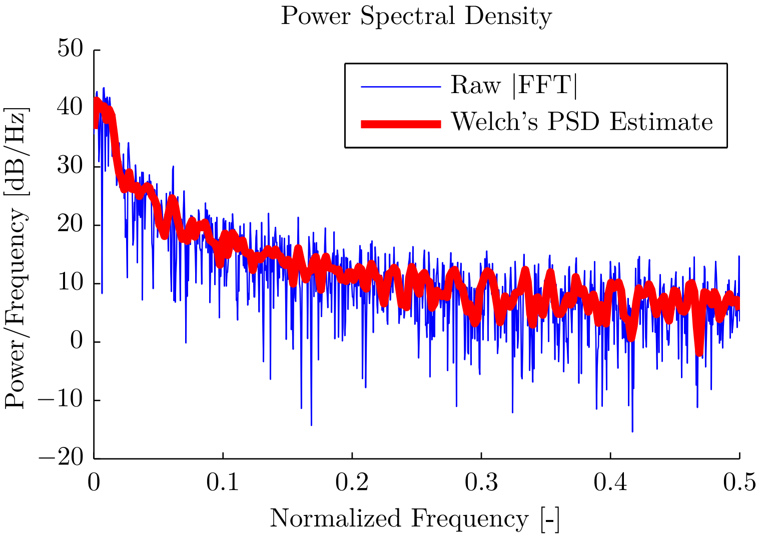

Figure 9: The Power Spectral Density of the PRBS

Another important point to mention is the difference between the signal's property of Persistent Exciting and its Power Spectral Density. Even though a signal could have a PSD that is non-zero for all frequencies, it does not necessarily have to be PE of high order.

For example, consider the Dirac Delta (an impulse) and the Heaviside function (a step signal). The spectral densities $\Phi_\delta(\omega) > 0 \quad \forall\, \omega$ and $\Phi_H(\omega) > 0 \quad \forall\, \omega$, although the latter decreases exponentially. The covariance matrix $R$ from Equation 3.4.4 shows that the Heaviside function is PE of order $n = 1$. The limit of Equation 3.4.4 does not exists which means the Dirac Delta function is not PE of any order, even though both signals have spectral content over a large frequency interval. These types of FD input signals have therefore not been used for further experiments.

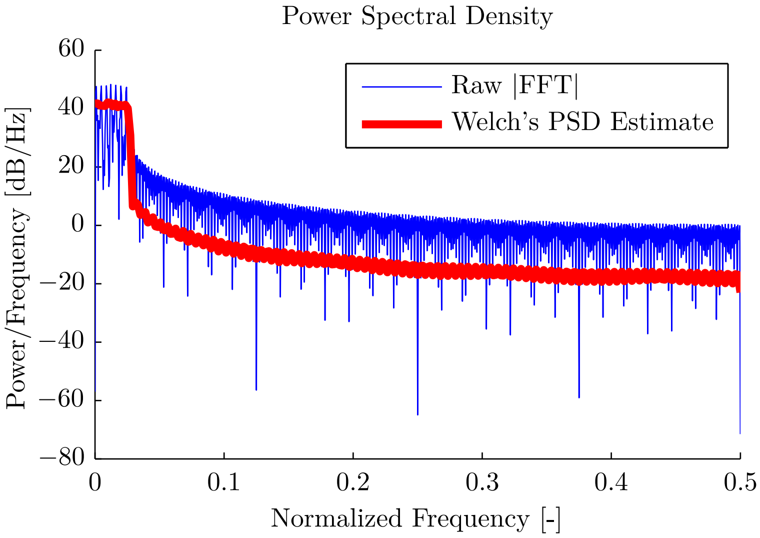

Figure 10: The Power Spectral Density of the multi-sine

### 3.4.7 *Dealing with multiple experiments*

The human pilot has been subject to more than one experiment. From literature, human control is know to be more or less linear against *unpredictable* signals [14]. The input signals for estimation and validation of the control model are identical. When asked, the pilots had not noticed the signals being the same. However, to avoid the learning curve of the pilot, for every experiment a new set of input signals is generated. By renewing the input pitch command, the human pilot is forced to respond as linearly as possible. The objective is to capture the pilot's pitch dynamics without the bias of the pilot getting used to the experiment.

### 3.4.8 *Remarks*

The design of the reference signal is of significant importance for the results of the system identification experiment. In general, designing the input reference signal is a trade-off between system identification requirements and the capacity of the pilot's control. From system identification theory, one would like a broadband signal with high signal to noise ratio. Unfortunately, this is only possible till a certain extend due to the limitations of human control (Figure 11).

## 3.5 DISTURBANCE INPUT

As described earlier in Chapter 2, the experiments are conducted in excellent flying conditions. There is no wind and no turbulence and aircraft (longitudinal) dynamics will be unaffected by external factors. Thrust levels, landing gear and secondary control surface settings will

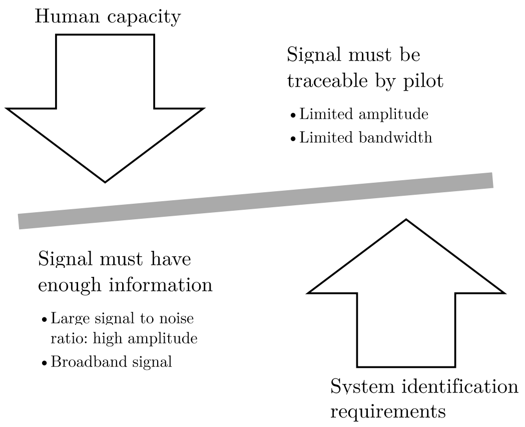
Human capacity
Signal must be traceable by pilot
• Limited amplitude
• Limited bandwidth
Signal must have enough information
• Large signal to noise ratio: high amplitude
• Broadband signal
System identification requirements

Figure 11: Illustration of the trade-off between human pilot limitations and system identification requirements for the FD reference input

be considered as initial conditions and do not affect the dynamics during the experiments. Furthermore, only pitch motion will be considered, other degrees of freedom will be ignored. Consequently the disturbance input can be assumed to be non-existent. The only 'disturbance' in the system is the human inherent noise as described by [30] and obviously cannot be eliminated.

## 3.6 HUMAN SUBJECTS

For the execution of the experiments, several 'pilots' have been asked to participate. Appendix E provides an overview for each subject. The subjects did not train a priori to the experiments, only a short briefing was given to explain the pilot's task. The pilots were not forced to be highly motivated (e.g. though a competitive element or monetary reward), although their performance was monitored and fed back after every session.

## 3.7 OVERVIEW

An overview of the three experiments can be found in Figure 12. It shows the simulated aircraft models and controlling pilots for every experiment.

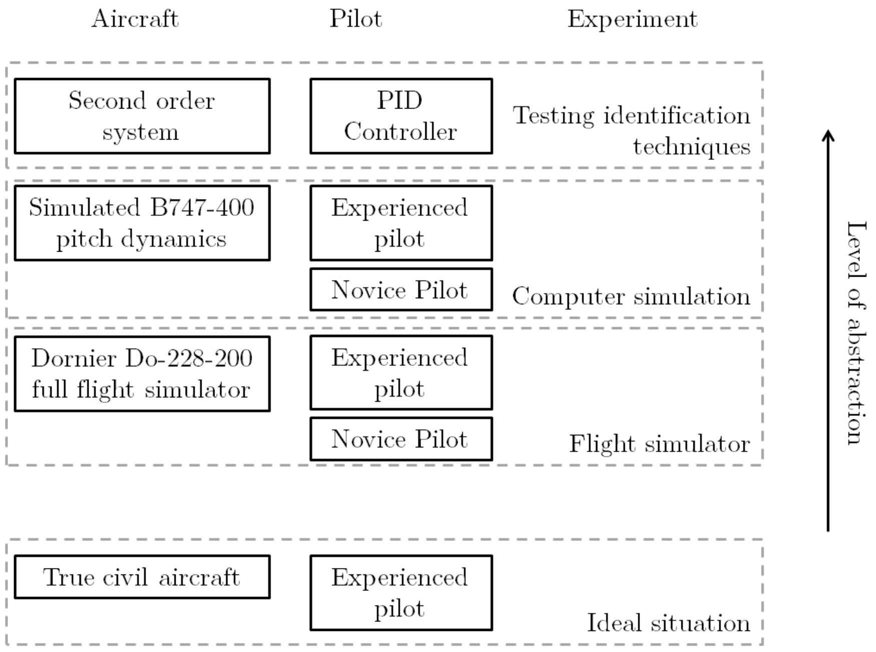

Figure 12: An overview of the three identification experiments

# 4 ANALYSIS OF RESULTS

This chapter elaborates on the results of the experiments from Chapter 3. Due to the large amount of data acquired, only the *(JAXA) Flight Simulator Experiment* will be analysed in this report. Identical procedures could be carried out for the other data-sets but in order to limit the number of analyses in this report, the focus will be only on the experiment with the lowest level of abstraction. Unfortunately, little is known a priori about the model's structure, order and control delay [33]. Therefore, several predictive models have been generated and evaluated on the availability to capture characteristic dynamics from the data, the Root Mean Square Error (RMSE) and the calculation time. Figure 13 shows the typical data obtained from the flight simulator experiment: the FD reference input which the pilot aims to track, the pilot's control input through the elevator and the actual pitch of the aircraft as indicated on the AI.

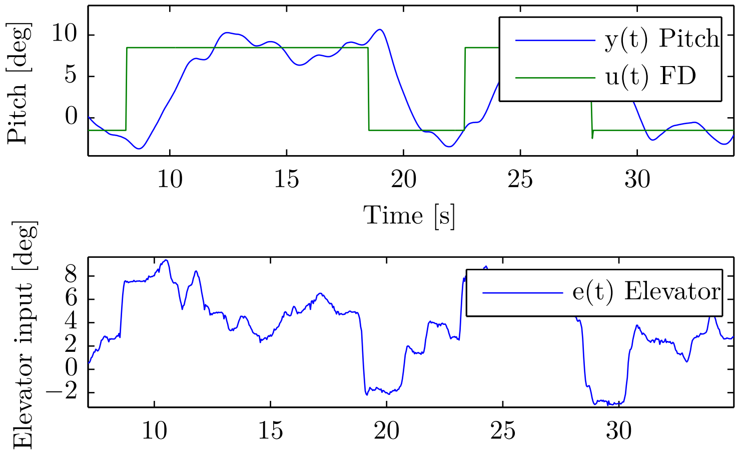

Figure 13: Typical data obtained from the flight simulator experiment. The reference input $u(t)$, control input $e(t)$ and pitch output $y(t)$ are recorded

## 4.1 CLOSED-LOOP BEHAVIOUR

The pilot is asked to track the movement of the FD. The actual pitch of the aircraft is provided to pilot through the AI on the PFD. This implies a feedback loop as depicted in Figure 14. The behaviour of this closed-loop system can be investigated.

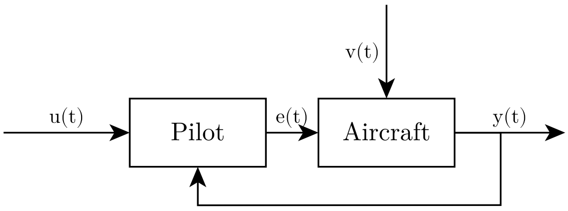

Figure 14: The closed-loop system

### 4.1.1 *Model structure*

As described in Chapter 1, a simple model that represents all significant system dynamics is preferred. in the field of system identification, models from the Auto Regressive, Moving Average (ARMA)-family are well-know structures and widely used in literature. The closed-loop system behaviour is modelled using the ARX model set. The main reasons for this choice are the number and the linearity of parameters. Note that although the parameters are linear, a ARX model can describe non-linear functions. The ARX parameters can be calculated quite conveniently through a least-squares algorithm (the PEM is a minimization problem), see Appendix A.

### 4.1.2 *Pre-processing*

System identification is performed on each dataset. The data has been removed of its means and is de-trended. The FD reference has mainly low-frequency content so pre-filtering is not necessary. Hence, it is split up into an identification and validation dataset.

### 4.1.3 *Model selection*

Human operators inherently have a reaction time delay. The time between the visual feedback of the aircraft pitch relative to the position of the FD and the corresponding control action is investigated in Appendix D. A minimum delay of 0.28 seconds can be expected, which translates to 7 samples of delay in the data.

The MATLAB `ident`-toolbox and GUI were used for model selection. A brute-force search method has been applied to find suitable ARX models with complexity in the range of 1-15 poles, 1-15 zeros and 5-15 sample delays. First, the model with the lowest Akaike Information Criterion (AIC) value has been selected, which describes a trade-off between model complexity (the number of parameters) and the goodness of fit (see Appendix A).

The model can be over-parametrized. Therefore, the parameters of $A$ and $B$ with a variance of the same order of magnitude as the parameter itself have been removed. A high parameter variance indicates that the

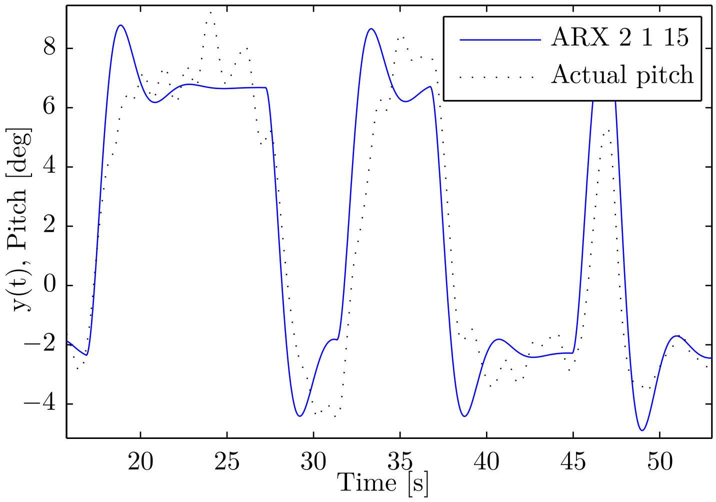

Figure 15: The ARX 2,1,15 closed-loop predictions versus the actual pitch $y(t)$

parameter might be redundant. Additionally, pole-zero cancellations have been eliminated. This results in a simplified ARX 2,1,15 model (Figure 15):

$$A(z)y(t) = B(z)u(t) + v(t) \tag{17}$$

$$A(z) = 1 - 1.938\, z^{-1} + 0.9431\, z^{-2} \tag{18}$$

$$B(z) = 0.00425\, z^{-15} \tag{19}$$

### 4.1.4 *Model validation*

Once the model is constructed, it can be used to predict the output. A 'perfect' model will exactly predict and overlay the measurement data. In reality, the difference between the model prediction and the actual data (called model residuals) are errors due to the order of the model, nonlinear effects and the limited number of samples. Therefore, the models need to be validated, which means it is tested if the models describe all significant dynamics from the experiment data. This can be done with the normalized autocorrelation test [28]. The autocorrelation of the residuals are defined as:

$$R_{ee}(i) = \frac{R_e(i)}{R_e(0)} = \frac{\frac{1}{N}\sum\limits_{t=1}^{N-i} e(t)e(t-i)}{\frac{1}{N}\sum\limits_{t=1}^{N-i} e(t)^2} \tag{20}$$

$$i = i_{max}, ..., 3, 2, 1, 0, -1, -2, -3, ..., -i_{max} \tag{21}$$

If the number of samples $N$ is large, $R_{ee}(0) = 1$. If $R_{ee} = 0 \forall i \neq 0$, the errors are said to be uncorrelated, meaning the model captures all the dynamics in the data. In practice, it is tested if

$$|R_{ee}(i)| \leq \frac{\delta}{\sqrt{N}} \qquad \forall i \neq 0 \tag{22}$$

with $\delta$ defining the level of significance. If this inequality holds, one can argue that the model residuals are from a Gaussian distributed white noise process, and past and future errors are not correlated. The model describes the 'noise' sufficiently well.

A similar procedure can be followed to analyse the normalized cross-correlation:

$$\begin{aligned} R_{ue}(i) &= \frac{\frac{1}{N}\sum\limits_{t=1}^{N-i} u(t)e(t-i)}{\left[\left(\frac{1}{N}\sum\limits_{t=1}^{N-i} e(t)^2\right)\left(\frac{1}{N}\sum\limits_{t=1}^{N-i} u(t)^2\right)\right]^{\frac{1}{2}}} && (23) \\ i &= i_{max}, ..., 3, 2, 1, 0, -1, -2, -3, ..., -i_{max} && (24) \end{aligned}$$

and

$$|R_{ue}(i)| \leq \frac{\delta}{\sqrt{N}} \qquad \forall i \neq 0 \tag{25}$$

This tests if the input is uncorrelated with the errors meaning that the model describes the output sufficiently well, i.e. the input is independent of the model residuals.

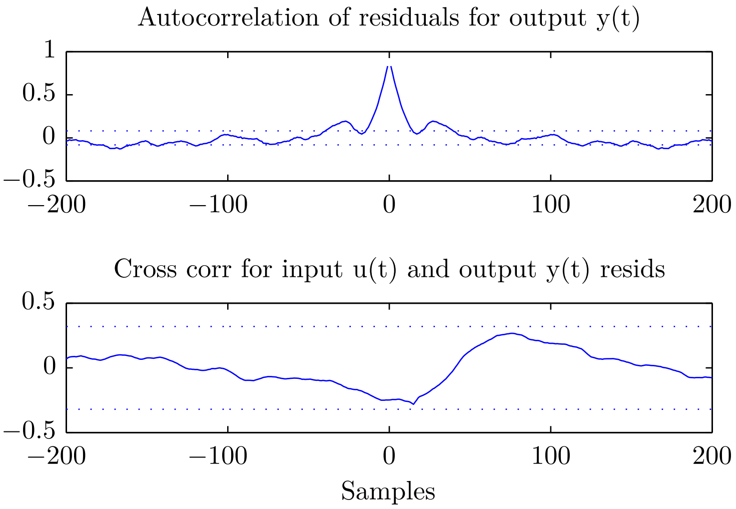

Figure 16: Correlation analysis for the closed-loop linear parametric model ARX 2,1,15. The auto-correlation plot indicates that the noise model can be improved. However, the cross-correlation stays within the 1% confidence interval: the model predictions of the output are acceptable.

In Figure 16 the autocorrelation and the cross-correlation plots are shown. For the model validation of the closed-loop model, a 1% confidence interval is used ($\delta \approx 12.7$, calculated with the `ident`-toolbox). The confidence interval is bounded by the horizontal dashed lines. As can be seen, the correlation analysis plots stay within this confidence region. The model prediction of the output is acceptable.

### 4.1.5 *The effect of experience*

For all sessions of the Flight Simulator Experiment, an ARX model can be made through the method described above. It might be interesting to see the difference between a novice and an expert pilot, from a control perspective. For both types of pilots, the closed-loop dynamics are evaluated by the model's frequency response (Figure 17).

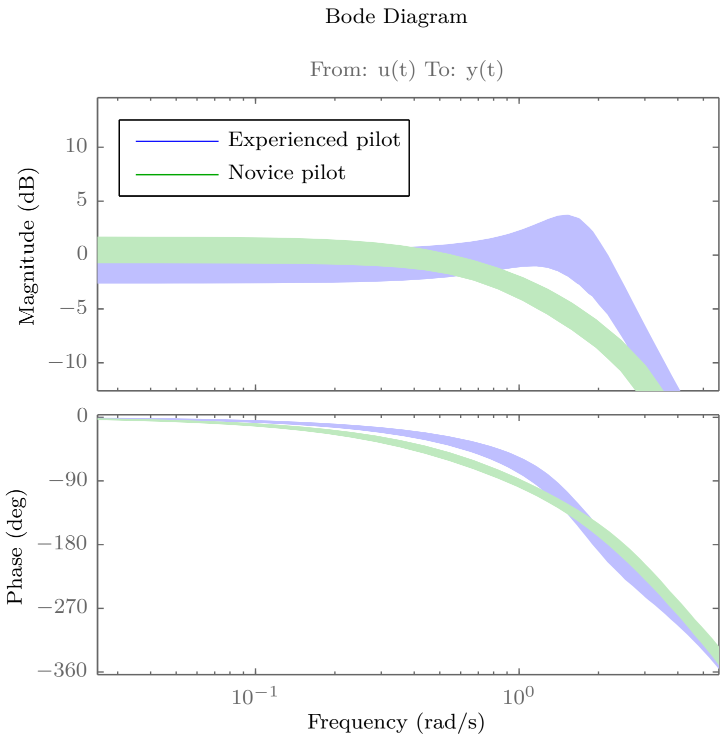

Figure 17: The frequency response from the experienced pilot compared to the novice pilot. The response is similar, but the experienced pilot has a higher closed-loop bandwidth. The area of the Bode-plot is due the parameter variances of the ARX model-set ($2\sigma$-bound)

.

One can see the low- and high-frequent characteristics are similar. The main difference is that the closed-loop bandwidth of the expert pilot is higher than the novice pilot. This phenomenon is supported by literature and can be explained by the difference in experience (it can be modelled for instance through the adaptive control 'windsurfer approach', briefly discussed by [15]).

## 4.2 HUMAN CONTROLLER DYNAMICS

One of the downsides of analysing the closed-loop behaviour is that the aircraft dynamics is in the model-set. This means that not only the human pilot control is captured, but also the specific aircraft the pilot is controlling. There are several ways to circumvent this problem and can be categorized under closed-loop identification techniques. Several methods are described by [17, 20, 15], but the *direct identification* method seems to be the most straightforward approach. As described in Appendix A, it is the starting point for any closed-loop identification task. The direct identification method simply ignores the feedback loop, which makes it possible to use well-established open-loop identification techniques. In this section, the a few approaches to model human controller dynamics are examined.

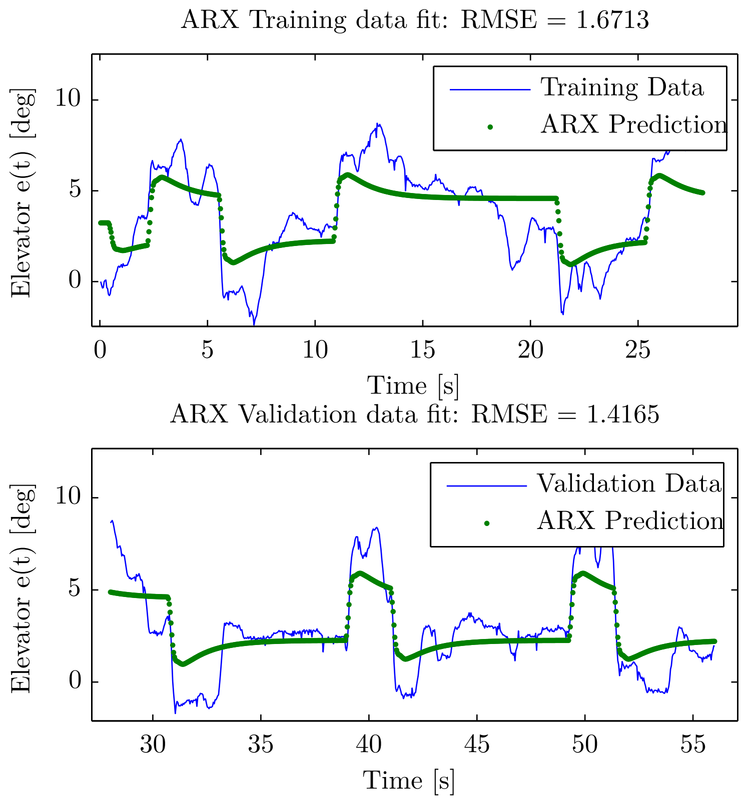

Figure 18: Pilot elevator control predicted by the ARX 9,6,10 model. The model doesn't capture corrective control and is more or less an average of the pilot's response.

### 4.2.1 *Linear modelling*

Similar to the modelling of the closed-loop, an ARX model structure is tested. The experiment data has been treated in similar manner: the data is de-trended and its means are removed. Furthermore, the data has been split into a identification and validation set. The least-squares adjustment of ARX parameters are brought to a halt using the AIC.

In Figure 18, the target signal, human response and model prediction have been depicted. As can be seen, the linear parametric model captures the human response to excitations of the PRBS target signal, but not the 'correcting' oscillating behaviour just after a target step. Instead, the linear model more or less mimics the average of the human response. The model accuracy is not particularly good because of this characteristic: the ARX 9,6,10 has an RMSE of 1.42. The model can be calculated in 0.72 seconds.

A sensitivity analysis on the ARX parameters has been performed. The number of parameters could be reduced in order to obtain a model with approximately the same accuracy and transient behaviour. The ARX 3,1,10 model can be found in Figure 19.

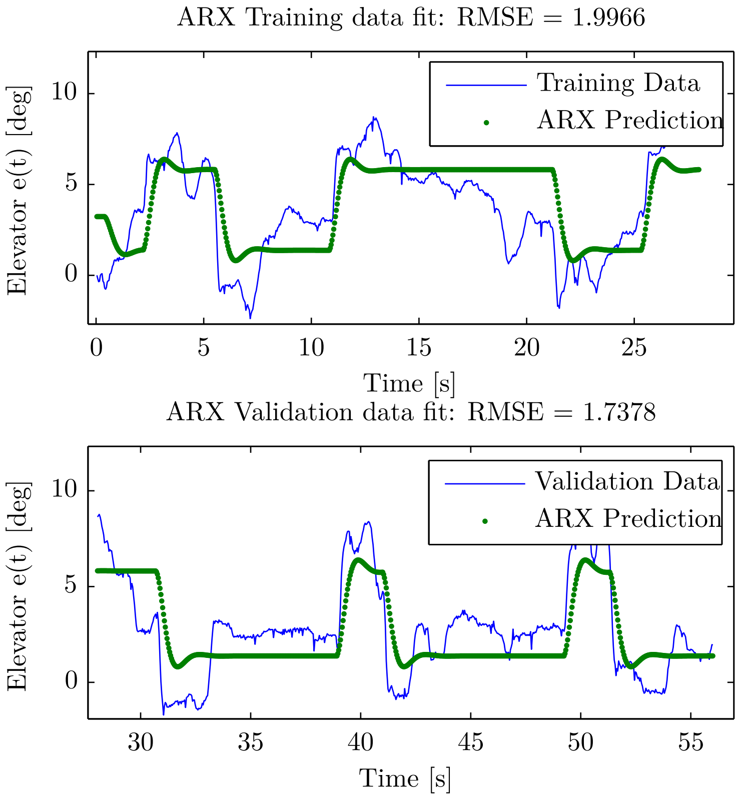

Figure 19: Pilot elevator control predicted by the simplified ARX 3,1,10 model. It has approximately the same response as the ARX 9,6,10 but less parameters

Model validation techniques reveal that the prediction residuals cannot be considered white so the model doesn't capture the human controller dynamics completely (Figure is not shown as it doesn't provide additional information). The frequency content of the residuals can be investigated through a PSD. However, all the periodograms rely on the Fourier transform. Since the residuals are stochastic, and not periodic, these fft-based methods might estimate the PSD wrongly. A high-order Auto Regressive, Moving Average, with exogenous input (ARMAX) model can be fit to the residuals to test the dynamics that remain unmodelled [5]. See its power spectrum in Figure 20.

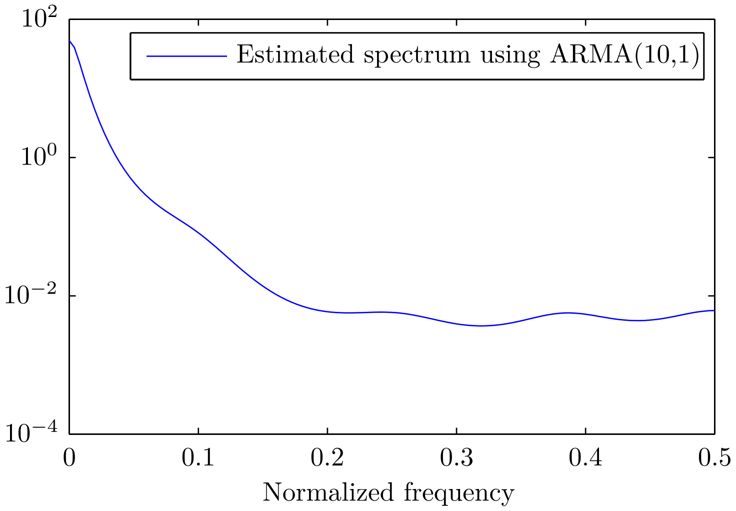

Figure 20: The PSD of the ARX model residuals, indicating that still low-frequency control action has not been modelled.

### 4.2.2 *Non-linear modelling*

Due to the non-linearities and the inherent noise of the human controller, it might be possible to obtain better results with a non-linear model set. In this report, the Neural Network and Adaptive Neuro-Fuzzy Inference System will be evaluated.

*Neural Network*

The Non-linear ARX (NARX) can predict non-linear time series. It is a form of Neural Network which includes a feedback connection within the network. The NARX model is inspired by the ARX model described above.

The Neural Network (NN) is good in describing time series. It can approximate any continuous non-linear function with arbitrary precision. This is called the *universal approximation theorem* [21]. However, a neural network can be considered as a black box in the sense that its structure will not provide any insights of the process that is being approximated. Neural networks are made to see whether system identification techniques related to the field of artificial intelligence could derive ‘better’ models from the data (in the sense of model fit and complexity, calculation time and describing control characteristics of the human pilot), compared to the ARX model set discussed previously.

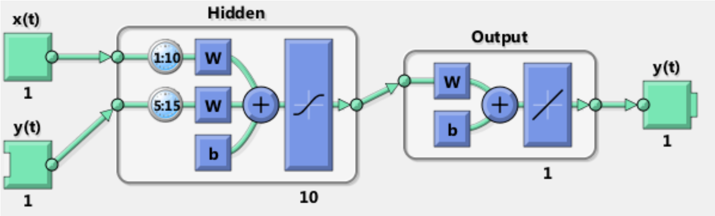

Figure 21: Neural Network NARX model structure

The NARX neural network consists of a hidden layer and an output layer. Both layers have weights and biases, with a sigmoid transfer function in the hidden layer and a linear transfer function in the output layer. Entzinger [12] gives a general introduction to neural networks. The network architecture is set as in Figure 21. The input of the network is the FD signal $u(t)$, the output is the elevator control $e(t)$. The NARX model set includes a feedback loop and will base its predictions of the elevator control on:

$$e(n) = \mathrm{NN}(y(t-5), ..., y(t-15), x(1), ..., x(t-10)) \tag{26}$$

The delays in the hidden layer is due to the expected human reaction time delay (Appendix 4) and consists of 10 hidden neurons. The output layer consists of only one neuron.

The experiment data is randomly divided into three sets:

- 70% training data
- 15% validation data (in order to prevent overfitting of the network)
- 15% independent checking data (in order to test the network's prediction performance on 'new' data)

In contrast to the linear ARX model, the data is not pre-processed due to the fact that the neural network can approximate the data regardless of biases such as trends and means. However, the data has been normalized as it can speed up convergence of the neural parameter values.

The weights and biases of the neurons are initially set to a random value. They are adjusted iteratively by a non-linear least squares solver called the Levenberg-Marquardt backpropagation algorithm - a rather common curve-fitting algorithm in literature. It will try to minimize the model prediction error by adjusting the neural parameters. Training will be brought to a halt when the model doesn't improve any more (checked by the validation data). See Figure 22. for the training progress. Like many other non-linear solvers, the algorithm might not find the global minimum. An optimal and unique solution therefore will not be found, as discussed in Chapter 6.

Figure 23. shows the human elevator response to the FD and the neural network prediction. The NARX neural network has excellent model fit (RMSE = 0.69) and can be calculated in 4.0 seconds. However, the model does need 261 parameters to achieve this result. Besides, the model allows elevator feedback which might result good predictions but

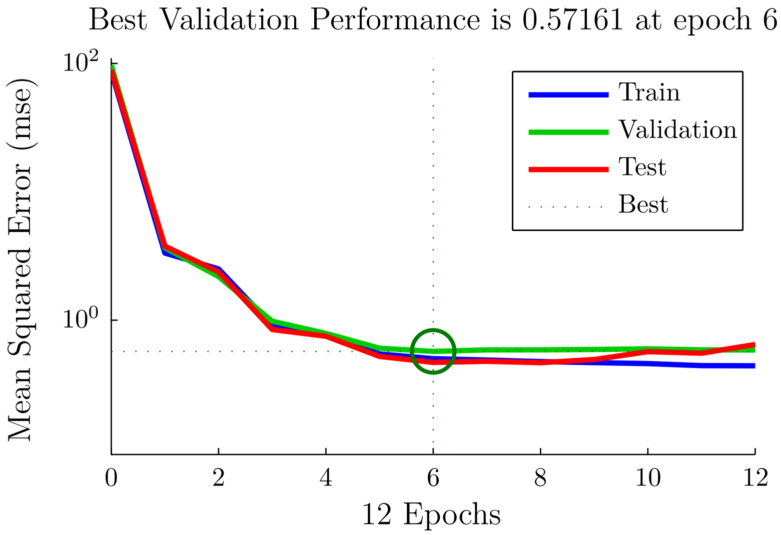

Figure 22: Training, validation and testing progress for the Neural Network

with a poor prediction horizon (a *naive predictor*). More on this in the next section and in Chapter 6.

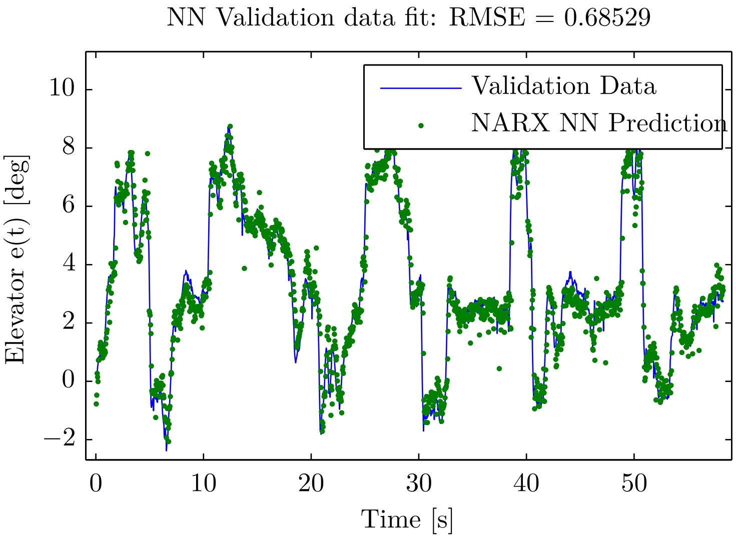

Figure 23: Pilot elevator control predictions by the NARX Neural Network. The predictions are close to the actual aircraft pitch $y(t)$.

### *ANFIS*

The ANFIS model uses methods from both Neural Networks and Fuzzy Logic. Similar to Neural Networks, ANFIS models have the capacity to describe any non-linear function with arbitrary precision. It can therefore describe a non-linear function better than any ARX model. It is able to 'train' in a similar way to NNs but with a fewer number of parameters. Fuzzy Logic is a form of logic that doesn't solely rely on 'true' or 'false', but can have any 'truth value' in between those extremes. Its power lies in the interpretability of the inference system. For a brief introduction to ANFIS, see Appendix A.

A Sugeno-Takagi fuzzy system is used which is in the form of fuzzy IF-THEN rules, described by [48]. Fuzzy logic relies on membership functions, which are essential to describe the 'partial truth' of a fuzzy system. Gaussian type, bell-shaped membership functions have been used in this research. These MFs ensure a smooth, continuous and differentiable fuzzy model.

The experiment data is split into a training and validation set and the data hasn't been pre-processed (unlike ARX models). The ANFIS membership functions are shaped and shifted until they fit the training data. This is a non-linear problem and can be solved with a gradient descend algorithm. The Sugeno-Takagi fuzzy system itself is a linear system, which parameters can be found using the least-squares method. The trained ANFIS consequently has 'linear' and 'non-linear' parameters. That is, the names indicate how the parameters are calculated. This method is called the hybrid learning procedure.

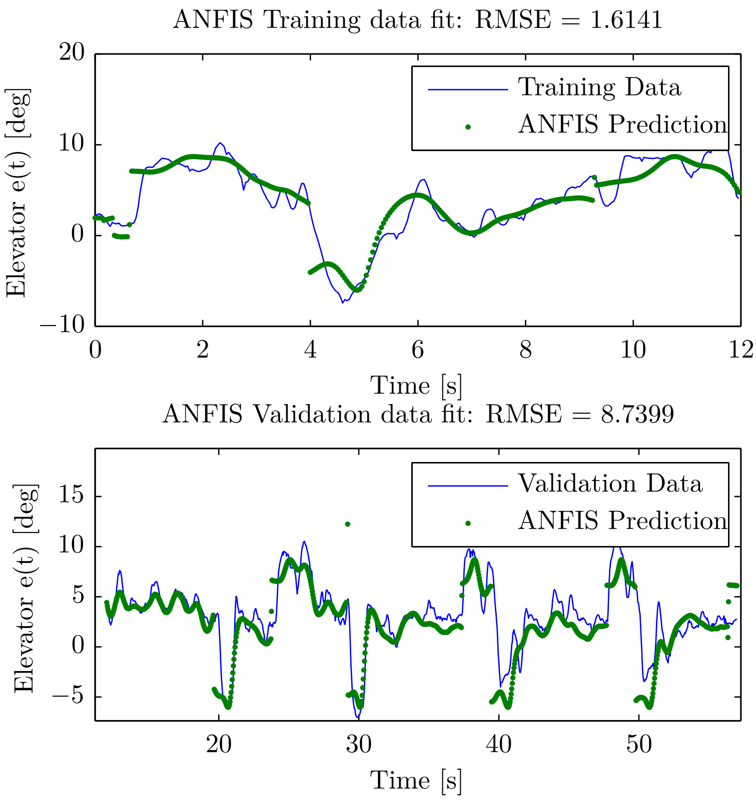

Figure 24: Pilot elevator control predictions by the ANFIS. Some large outliers are not shown in the plot.

The number of Membership Functions (MF)s, along with the number of model inputs define the complexity of the ANFIS. There are $m^n$ fuzzy rules trained, with $m$ the number of MFs and $n$ the number of inputs. As for all models, typically, the more parameters are introduced, the better the model fits the data. A model with a small number of parameters is preferred, so initially the number of MFs is set to 2. The output MF is constant.

From a system identification perspective, it makes sense that the human operator is influenced by the FD reference input (Figure 14). Furthermore, the pilot can evaluate the actual aircraft's pitch to adjust its control action, which makes the pitch data also a model input. One can argue that there can also be an elevator feedback loop. This would mean, that the (time delayed) elevator data is treated as a model input as well as the model output. Physically, it means that the pilot 'knows' his previous control input and adjusts his next input accordingly. Although it is plausible in reality, it can lead to erroneous results when this is tried to be modelled using the ANFIS model set[1]. See the discussion in Chapter 6 on feedback channels. Therefore, in this report, the ANFIS will only have pitch feedback in its search space.

The model inputs are subject to various time delays, such as human response time and delay due to system inertia. For the calculation of the elevator output at any sample $n$, the delayed versions of the input and output data are used:

$$u(n-1), u(n-2), u(n-3), ..., u(n-q) \tag{27}$$

$$y(n-1), y(n-2), y(n-3), ..., u(n-r) \qquad q, r << N \in \mathcal{R} \tag{28}$$

with $u$ the FD input, $y$ the actual aircraft's pitch and $N$ the total number of samples.

A sequential search algorithm is used to find the optimal model inputs with respect to the model's RMSE and $u(n-9)$ and $y(n-4)$ have been selected. The danger of a sequential search algorithm is that it might converge to a local minimum. A brute force algorithm is a solution, but takes significantly more computer power.

Similar to the discussion in Section 4.1, there is an indication that experienced pilots have different control dynamics compared to novice pilots. The sequential search algorithm provides the model inputs for which the model output has the lowest RMSE and is given below:

$$e(n)_{expert} = \text{ANFIS}\left(y(n-3), u(n-11)\right) \tag{29}$$

$$e(n)_{novice} = \text{ANFIS}\left(y(n-3), u(n-9)\right) \tag{30}$$

Although a further comparison of the models can be performed, only the model of the expert pilot is considered. The elevator output of the ANFIS is shown in Figure 24. The high RMSE is due to large outliers in the model prediction. They occur at the sudden change in FD command due to the sharp, binary character of the PRBS. Although the RMSE of the ANFIS is high, the model does capture some human control dynamics in detail. Some essential control characteristics are predicted[2].

[1] The ANFIS can generate a 'naive predictor'

[2] Note that similar results as the NN can be achieved when the ANFIS includes the elevator feedback in its search space (see Chapter 6). In order to avoid 'naive predictions', this is not done.

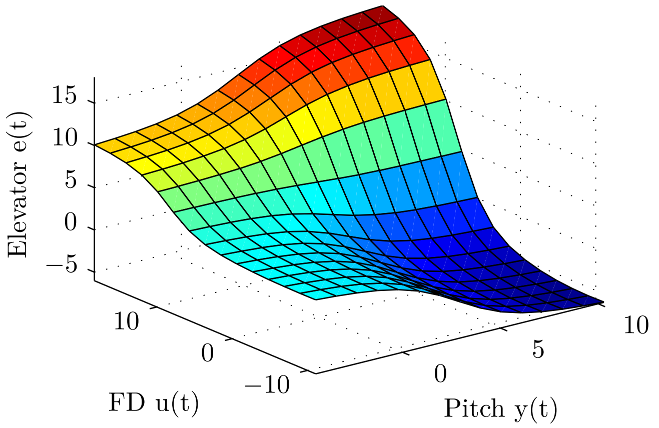

Figure 25: The control surface of the ANFIS. Note the non-linear relation between the elevator output, the FD input and the aircraft pitch.

Furthermore, the output surface of the model is shown in Figure 25. and clearly shows non-linear relations between the inputs and the output. Note that although locally linear surfaces are within the ANFIS search space, it can be hard to achieve a such with Gaussian MFs. The surface shown Figure 25 can be compared to surfaces calculated with other MFs to evaluate the non-linearity. This is left for further research. The fuzzy rules and 'trained' membership functions are depicted in Figure 26. The ANFIS can be calculated in 0.55 seconds and has 4 rules and 16 parameters.

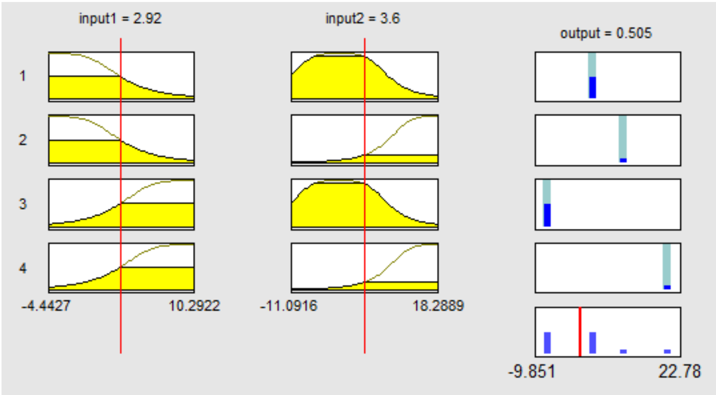

input1 = 2.92

input2 = 3.6

output = 0.505

Figure 26: Four fuzzy rules of the ANFIS with Gaussian bell shaped MFs on the two inputs

### 4.2.3 *Overview*

Table 3 gives an overview for the RMSE, number of parameters and calculation time of the selected models. Some remarks have been made concerning the dynamic response of the system. Furthermore note that the modelling techniques used in this chapter are generally used to

| | ARX | NN | ANFIS |
|---|---|---|---|
| RMSE | 1.74 | 0.66 | 8.74 |
| Number of parameters | 4 | 261 | 16 |
| Calculation time | 0.72 | 4.0 | 0.55 |
| Remarks | Simple linear-in-the-parameters model | Note the elevator feedback of the NARX model-set | Interpretable fuzzy rules. Outlying predictions at PRBS switch |

Table 3: Overview of the pilot elevator control models

identify plant behaviour in literature. In this case, attempts have been made to identify the controller and the same system identification algorithms have been used for this purpose.

# 5 CONCLUSION

This internship report describes the contribution to the research project on the safety of curved approaches at The University of Tokyo, Department of Aeronautics and Astronautics. This work focusses on:

- Investigating closed-loop dynamics of pilot-aircraft interaction
- Determining a suitable model-set to capture human pilot pitch control dynamics.

Three experiments have been designed where the pilot is requested to track the FD reference signal. The yoke control input and aircraft's pitch are recorded. Data from the JAXA full flight simulator experiment is used for the analyses in this report.

From system identification theory it is known that the input signals require certain characteristics in order to estimate consistent models. Properties like the duration of the experiment, sample time, signal-to-noise ratio and persistent excitation of the signal influence the quality of the reference signal for identification purposes. However, due to the limitations of the human operator, not all broadband signals are suitable. The selection of the input signal is a trade-off between the system identification requirements and the capacity of human control. It is shown it is possible to design such signals within the human control bandwidth. During the experiments, the PRBS is used as FD reference input.

The human-aircraft system contains a visual pitch feedback loop. The closed-loop dynamics can be modelled by a linear-in-the-parameters ARX model and correlation analysis shows that the model predicts system characteristics sufficiently well. In frequency domain, models from experienced versus novice pilots indicate a difference in closed-loop bandwidth. It is hypothesised that experienced pilots typically have a higher bandwidth than novice pilots. Further research is needed to validate this concept, but it is in agreement with characteristics of human operators in literature.

In order to distil the human controller dynamics from the closed-loop configuration, the direct system identification approach has been used. The linear parametric ARX model captures the basic control dynamics at the switch of the PRBS, but does not include corrective control.

The 'intelligent' non-linear model set, NARX Neural Network has an excellent model fit but requires many parameters (computationally expensive) and relies on elevator feedback.

A neuro-fuzzy solution has been introduced. The ANFIS model has significantly less parameters than the neural network and relies on delayed FD input signals and current aircraft pitch. Although the model fit is less than the other controller models, it does capture the pilot's corrective control. The ANFIS consists of (only) 4 linguistic rules and interpretation is straightforward compared to neural weights and model parameters.

Similar to the closed-loop analysis, there is an indication that the level of piloting experience is distinguishable with respect to controller dynamics.

In general, system identification techniques can be valuable analysis tools for further research on modelling the human pilot control strategy. Within the project on the safety of curved approaches, but also research on other flight phases and procedures, transient and frequency response could provide insights on pilot capacity and performance.

# 6 DISCUSSION AND RECOMMENDATION

This chapter discusses the experiment design, several aspects of human pilot modelling and possible applications. Furthermore, recommendations for further research are given.

## 6.1 EXPERIMENT DESIGN

This report only focusses on pilot pitch control. In Chapter 3 the experiment setup is explained. The reference signal of the FD is a PRBS and has been tuned to fit the needs for system identification while remaining traceable by the pilot.

The input signal is not a realistic FD signal which - under normal conditions - changes gradually. It is known that human operators can change their control strategy according to the task and at any moment. It is therefore possible that the models in this report represent the pilot pitch control for this experiment setup specifically, and not in general. In further research, one could choose not to override the FD, but to use it as is during the experiment. The implementation of a curved approach is then possible. The problem is that the FD would probably not be PE so linear parametric models will not provide consistent results. 'Intelligent' modelling (ANFIS or NN) remains possible as they do not require the PE property.

The input signals in the report are designed to have frequency content within human bandwidth. Theoretically, this limits the validity of the model up to that bandwidth and is true for the multi-sine signal. It is lesser of a problem for the PRBS. Due to the square-wave properties, the PRBS has more high-frequency content. Pool et al. [40] present methods to obtain a wide-frequency-range pilot control model.

In Chapter 4, it is discussed that there is an indication that the experience of the pilot can be observed in the closed-loop and controller model. Novice pilots tend to show a lower closed-loop bandwidth than the experienced pilot. It has not been tested if the bandwidth change is statistically significant. It can be tested by obtaining the bandwidths of multiple experiments and verify if the novice pilot in fact has a lower bandwidth than the experienced pilot, by for instance an Analysis of Variances (ANOVA).

## 6.2 PILOT MODELLING

Some remarks have to be made concerning the modelling of pilot control dynamics.

### 6.2.1 *Predictive versus causal modelling*

In this report, linear parametric ARX and non-linear 'intelligent' ANFIS and NN model-sets have been used to capture the pilot pitch control dynamics in a predictive mathematical model. It is tempting to think that a model that predicts the future output sufficiently well (in this report measured by the RMSE), also *explains* the underlying character of the system. This, however, certainly does not have to be the case. Shmueli [44]: This is due to "the fact that measurable data are not accurate representations of their underlying constructs. The operationalization of theories and constructs into statistical models and measurable data creates a disparity between the ability to explain phenomena at the conceptual level and the ability to generate predictions at the measurable level". For instance, consider an model $\hat{f}(x)$ that should model the observations $Y$ of a process. The expected prediction error can be defined as:

$$\begin{aligned} EPE &= E(Y - \hat{f}(x))^2 && (31) \\ &= \ldots && (32) \\ &= \mathrm{Var}(Y) + \mathrm{Bias}^2 + \mathrm{Var}(\hat{f}(x)) && (33) \end{aligned}$$

The Bias term is due to an erroneous model set $\hat{f}(x)$, the third term because of the use of sampled data to estimate $\hat{f}(x)$. The first variance is the error even when $\hat{f}(x)$ would be perfectly specified. Shmueli [44]: "In explanatory modelling the focus is on minimizing bias to obtain the most accurate representation of the underlying theory. In contrast, predictive modelling seeks to minimize the combination of bias and estimation variance".

The latter is done for all the models in this report. In fact, model-sets from the ARMA-family are solely suitable for predictive purposes. Also machine-learning type of models (including ANFIS and NNs) are usually constructed to minimize the prediction error. It can therefore happen that predictive mathematical models converge to a '*wrong*' explanatory model in order to obtain maximum empirical prediction precision.

### 6.2.2 *Feedback channels*

This is related to the issue of providing elevator feedback to self-learning model-sets. As discussed in Chapter 4, one should be careful in deciding which feedback channels to use for pilot control identification. The NARX NN shows excellent predictions based on FD input and elevator feedback. Similar, or even better results can be obtained with the ANFIS model structure with elevator feedback (Figure 27). However, its performance is only apparent. During the learning process of the ANFIS, the model developed into a *naive predictor*; a model that predicts only on its previous sample. Consider the observations $Y$ of a stochastic process. The naive prediction for the next time step $k$ is:

$$Y_{k+1} = Y_k + \epsilon \tag{34}$$

where $\epsilon$ is the prediction error of the model. When the sample time is very short compared to the dynamics of the to be identified system (which is the case in this report), the naive predictor will have an excellent model fit (i.e. a low RMSE).

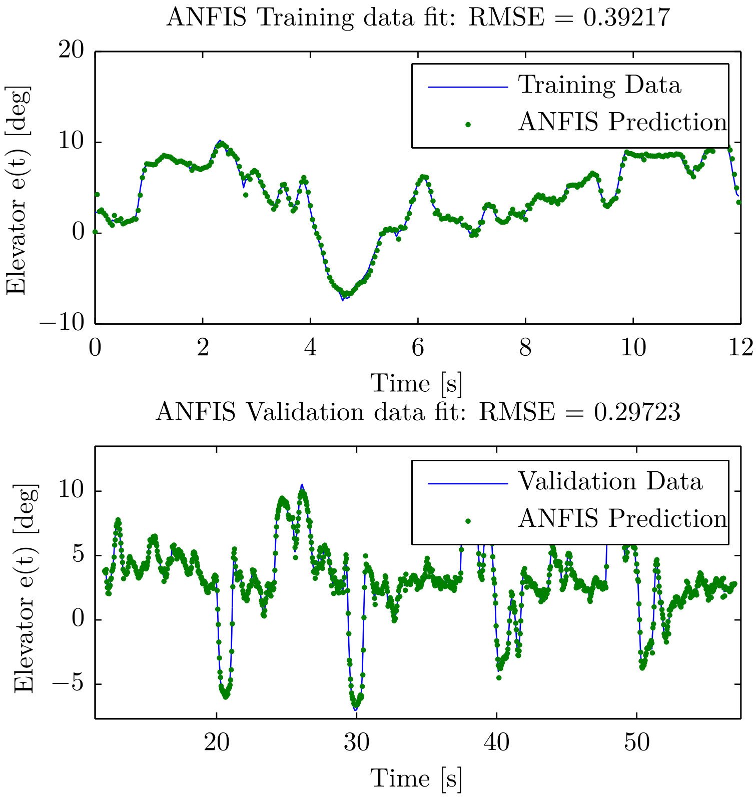

Figure 27: The naive predictions of an ANFIS with elevator feedback

The ANFIS and NN were not restricted to generate such naive models[1]. Due to the open, interpretable structure of the ANFIS, this problem was recognized. Therefore, in Chapter 4, the ANFIS model has been made with pitch feedback information only. The NN is more of a black box since its neural weights and biases are not easily interpreted. It is not certain the NN in Chapter 4 provides naive predictions, but it has been shown that the pilot's elevator control can be approximated with such non-linear model-sets. Furthermore it should be kept in mind that these 'intelligent' models provide no mathematically unique solution. This is in contrast with the linear parametric ARX model, under Persistent Exciting conditions[2].

One can argue such an elevator feedback loop does exist since any reasonably trained pilot 'knows' what the effect of pushing and pulling of the yoke is: it will cause respectively downwards and upwards pitch change. This is known even without observing the actual aircraft's pitch

[1] The naive predictor is in the search space

[2] This has to do with the concept of *identifiability*, see Söderström and Stoica [45]

on e.g. the AI. It is not affected by visual reaction time delay and therefore introduces as the *'fast loop'*. As depicted in Figure 28, this implies a feedforward path. In order to track the FD signal, the pilot should behave as the inverse of the aircraft dynamics. This idea is supported by research by Laurense et al. [27]. The quality of this feedforward inverse model can be evaluated by the pilot's tracking performance. Errors in the feedforward path (so mistakes in the controller dynamics) can be corrected using the slower visual feedback loop with the pilot looking at the actual pitch on the AI.

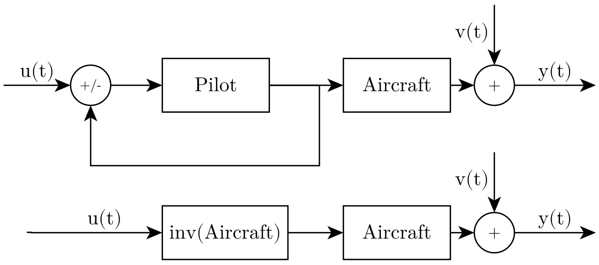

Figure 28: Elevator feedback implies the pilot behaves as the the 'inverse of the aircraft'. The block diagrams are similar.

Further research also has to clarify the effect of feedback of the pitch rate $\frac{d\text{Pitch}}{dt}$. The indication of the aircraft's pitch and pitch rate are inextricably linked on the PFD and the pilot is likely to base its control strategy on this information too.

For pilot control analysis, it might be useful to identify feedback loops from the explanatory perspective and developing predictive models from that starting point. Causality can be tested with series of statistical methods[44]. This would result into a more solid theoretical framework of pilot (pitch) control and could improve the performance of the predictive models.

### 6.2.3 *Multidimensionality of aircraft control*

Expanding the human pilot control model can be rather challenging. Some ideas for the further development of a pilot control model have been presented.

This report is on pilot pitch control. Perhaps one would like to investigate the roll or yaw control in the future. Composing the models in a control matrix, like proposed in Chapter 2 could result in a more complete model of the human controller. It is interesting for further research, however, it is questionable if this control matrix would mimic true pilot control as humans tend to change the control strategy according to task and several other factors.

Additionally, during regular manual operation, the pilot uses various cockpit instruments and many visual and motion feedback channels. The pilot will be scanning these instruments in a fixed or changing pattern over time [43]. For all these instrumental, visual and motion cues, one could identify models that map these inputs to the output states of the aircraft. Hence these models could be linked into a ‘switching’-model which changes system inputs, outputs and dynamics over time according to the scanning pattern. For identification, particularly switched parametric models like SARX and SS-ARX, are used in literature [18, 51]. Another way to link the pilot’s dynamic response from different instrument feedback is by making a fixed parametric model structure, but switching the parameter values according to the scanning pattern. This is shown in [6] using fuzzy parameter switching.

## 6.3 REMARKS ON OBSERVATIONS

During the experiments, there were some comments on the pilot’s pitch control that haven’t been discussed in detail. The human pilot shows high-frequent, push-pull control action in the FD tracking task. There might be several reasons for this strategy:

1. The yoke or elevator might have a dead-zone because of mechanical backlash. Consequently, parts of the pilot control action is not transferred to actual motion of the aircraft. The pilot will try to correct for this error. This reason seems less likely because the control dynamics remain similar even if flights are performed in simulators with hardly any backlash of the yoke (such as JAXA’s Dornier Do 228-200 full flight simulator). Also, the dead-zone could be taken into the model-set explicitly, as described by Wang et al. [53].

2. It might be easier to control the aircraft while there is pitch motion. The pilot will constantly adjust the aircraft’s pitch rate so it can anticipate on FD changes quicker. This ‘moving cursor strategy’ has already been recognized during a reaction time experiment of Mr. Uemura from the Department for Aeronatics and Astronautics at The University of Tokyo.

3. The pilot might be ‘impatient’ due to the high inertia of the aircraft. The response of a big commercial aircraft (like the simulated B747-400) typically is rather slow. The high-frequent elevator action averages out to low-frequent aircraft pitch motion (in a similar manner to Pulse-Width-Modulation in digital systems).

4. A more complex reason could be that the pilot performs on-line system identification to build a suitable ‘internal’ control model. Providing more high-frequencies could result in a better understanding of the aircraft’s dynamics. The model is contentiously adjusted to past experiences. Methods to model the pilot as an adaptive controller has been proposed by [39].

5. Another reason could be that it is more convenient to control the aircraft past the integrator $\frac{1}{\tau_i s}$ in frequency domain. In Appendix

C, the Bode plot of the B747-400 is shown. Controlling the aircraft with a frequency higher than approximately 1Hz could be easier as errors of higher than that frequency will not get magnified by the integrator. The pilot tries to avoid the low-frequency zone.

## 6.4 APPLICATION

This report covers system identification techniques after the data has been acquired. However, when the models are updated on-line and recurrently re-estimated, the proposed methods have the potential to provide the pilot predictions of its own control *in advance*. During operation, the models predict future control dynamics and could present instructions or warning messages based on the pilot's control. It can accelerate learning for novice pilots [33].

It is already possible to evaluate the pilot's control after the experiment flight by using the pilot identification methods in this report. The flight data from for instance the Suzuki-Tsuchiya laboratory B747-400 simulator can be logged. Previous work at the Department of Aeronautics and Astronautics resulted in tools to conveniently process the raw flight data to PSD diagrams and Bode plots. With some minor adjustments, the code in the Pilot Identification Toolbox for MATLAB can be an extension of the evaluation tools for pilot control.

# A SYSTEM IDENTIFICATION AND PARAMETER ESTIMATION - BACKGROUND

## A.1 SYSTEM IDENTIFICATION THEORY

System identification focusses on deriving a mathematical model of a dynamic system based on (experimental) observed input and output data [29, 1]. The identified model characteristics, accuracy and complexity can be defined by the user and model assessment depends on the application of the identification task. In this report only the outlines of will be reviewed because the field of subject is quite large. If the reader wants a greater level of detail, there are is a large collection of in-depth literature available, which is referred to in this review.

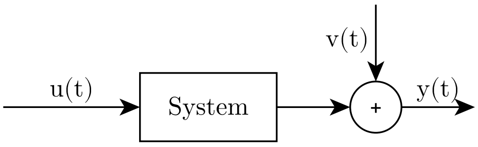

Figure 29: An open-loop system with an input $u(t)$, output $y(t)$ and disturbance $v(t)$

Consider the open-loop system in Figure 29. The system is subject to an input signal $u$ which can be recorded in time. The output signal $y$ can also be observed. However, the output can contain noise (disturbances or measurement errors), denoted by $v$ which means that the observed output is not directly caused by the input, but also by the addition of irrelevant information. System identification tools are used to estimate underlying system dynamics from only the recorded input and output recordings.

The core of estimating models originates from statistical theory. In general the identification problem can be described by the following features [29]:

- A (mathematical) model obtained from observed data. The data is usually influenced by system or measurement noise so estimation is not straightforward.
- The choice of a certain model structure
- The choice of a model complexity
- Estimation of the model with one part of the data set,
- Validation of the model with the other part of the data set,
- Performance measurement (e.g. by the model fit).

The identified model should resemble ‘reality’ as close as possible, with a certain accuracy defined the user. It should ‘explain’ the underlying mechanism that maps the input to the output. In short, “the model should show good agreement with the estimation data", and “the model should not be too complex" [29]. In Figure 30 the system identification process is explained by means of a flow chart.

Basic system identification generally considers Linear Time Invariant (LTI) systems, with sufficiently exciting[1] [1], sufficiently rich[2], wide-sense stationary[3] [26] input signals. It assumes that the observed output data are realizations of a stochastic process fed by the input. A remark has to be made concerning continuity. Since the data for system identification is captured during experiments, the data is usually measured at a fixed interval. This implies handling discrete data points in stead of continuous functions. Data collected at a high enough sample rate can of course be said to be ‘continuous’. Another remark that has to be made is that (open-loop) system identification only works when the input and disturbance signals are statistically uncorrelated (see Figure 29). That is why the disturbance generally is taken to be realizations of a white noise process. Ljung describes the core of the system identification theory as well as the application in his book [28], which can be considered as one of the field’s leading text books.

### A.1.1 *Non-parametric models*

*Non-parametric* models are estimated by correlation analysis of the input signals. This process is described by Aarts [1], Kwakernaak and Meinsma [26] and Ljung [28]. Although their notations are different, the method is similar:

- The auto-covariance of the input $r_u(\tau)$ and the cross-covariance $r_{yu}(\tau)$ are calculated by using more or less standard statistical techniques.
- These covariances can be Fourier transformed from which the spectral densities $\phi_u(\omega), \phi_{yu}(\omega)$ can be obtained.
- The frequency response system equation can be obtained by

$$\hat{G}_N(e^{i\omega}) = \frac{\phi_{yu}^N(\omega)}{\phi_u^N(\omega)} \tag{35}$$

This method is called the Emperical Transfer Function Estimate (ETFE). For this method to work properly in practice, usually smoothing is applied to the spectral densities, called *windowing*, because they often have “erroneous and irregularly fluctuating appearance” [26]. There

[1] The signal to noise ratio should be high enough in order to have accurate and consistent estimations.

[2] Sufficiently rich in this case means that the signal contains “all” frequencies. This can be evaluated for instance by a power spectral density plot.

[3] Wide sense stationary signals are signals that have the same stochastic properties in different time frame windows. That is, a constant mean and a constant variance over time.

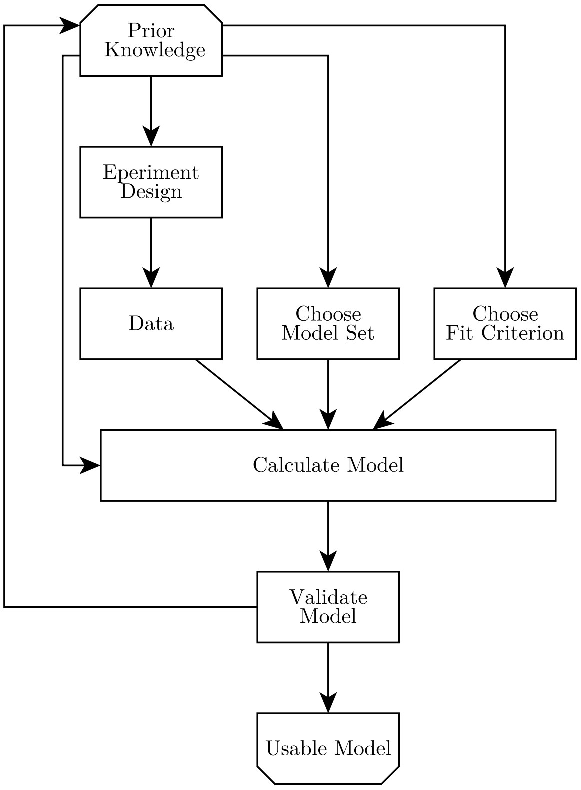

Figure 30: The system identification process [28].

are several was to do this, but a common windowing function is the Hamming window.

An alternative way to perform non-parametric system identification is the SPectral Analysis method (SPA). The method handles spectral densities a bit differently:

$$\phi_y^N(\omega) = |\hat{G}_N(e^{i\omega})|^2 \phi_u^N(\omega) + \phi_v^N(\omega) \tag{36}$$

with $\phi_v^N(\omega)$ calculated with the coherence spectrum $\kappa_N$. This is a measure from 0 to 1 of how much of the output is “explained" by the input and noise. This can be calculated so using SPA is solving for $\hat{G}_N(e^{i\omega})$.

Non-parametric models can estimate the system’s frequency response by using signal spectra. Model complexity can only be controlled by the amount of smoothing in the frequency domain. These models typically serve as guidelines for parametric models [1].

### A.1.2 *Parametric models*

Differently from the previous discussed non-parametric models, parametric models are designed to capture input and output relations in a certain, pre-defined structure.

*Prediction Error identification Method*

The idea behind the Prediction Error identification Method (PEM), is that a estimated system model performs well enough if it can predict it's own output based on a known input correctly (i.e. within a certain precision). It assumes that the sampled data can be captured in a finite order system[4]:

$$y(t) = G(z)u(t) + H(z)e(t) \tag{37}$$

where $e(t)$ is white noise. Hence, the model structure can, for instance, be written as a fraction of polynomials:

$$\begin{aligned} G(z,\theta) &= \frac{B(z^{-1},\theta)}{A(z^{-1},\theta)} && (38)\\ H(z,\theta) &= \frac{1}{A(z^{-1},\theta)} && (39)\\ A(z^{-1}) &= 1 + a_1 z^{-1} + ... + a_n z^{-n} && (40)\\ B(z^{-1}) &= b_1 + b_2 z^{-1} + ... + b_n z^{-(n-1)} && (41)\\ \theta &= [a_1, a_2, ..., a_n, b_1, b_2, ..., b_n]^T && (42) \end{aligned}$$

This is the ARX structure. Here, parameter estimation $\theta$ takes an important role in the system identification process. The parameters are found by minimizing the prediction error of the model, or by fitting the model in the least-squares sense. Which structure and what complexity is used depends on the application. Indicators such as residuals, and (root mean square) model fits help judging if the model fit is sufficiently accurate. On the other hand, information criteria like the Final Prediction Error (FPE) of Akaike indicate if an appropriate complexity is achieved.

There are many structures within PEM that model all kinds of system properties (different model set for $G(z,\theta)$ and $H(z,\theta)$). A few of them are listed below [1].

- ARX - Auto-regressive models with exogenous inputs
- ARMAX - Auto-regressive, moving average models with exogenous inputs
- OE - Output Error models
- FIR - Finite Impulse response models
- BJ - Box-Jenkins model structure

*Sub-space identification*

A discrete LTI system can be written in state-space format:

$$\begin{aligned} x(n+1) &= Ax(n) + Bu(n) && (43)\\ y(n) &= Cx(n) + Du(n) && (44) \end{aligned}$$

[4] Literature uses different notations to indicate the transfer function $G$. Another way is using the backward shift operator $G(q)$, which probably is more correct, mathematically [28, 26]

The transfer function is then given by

$$G(z) = D + C(zI - A)^{-1}B \tag{45}$$

The system to be identified is subjected to an impulse input. From the response, the Hankel matrix is calculated which contains enough information to calculate the matrices $A, B, C, D$ by a technique called singular value composition (SVD) [50]. The system is parametrized in four, finite length matrices. The advantage of using sub-space identification is that it is particularly well suited for MIMO problems [36].

## A.2 RECENT DEVELOPMENTS IN SYSTEM IDENTIFICATION

Previously described system identification techniques are considered well-known and can be used to solve a wide variety of identification problems [54]. In the next section, current research in identification theory and practice will be examined.

### A.2.1 *Closed-loop identification*

Although closed-loop identification has been a topic of interest for a while [28], it still remains to be an active research field. Consider Figure 31. Techniques as described in the Systems Identification Theory section only work when the input $u(t)$ is uncorrelated with $v(t)$. The feedback loop is needed for the controller to base its control action on. However, adding a feedback loop will immediately destroy the property of the signals being uncorrelated [26, 19].

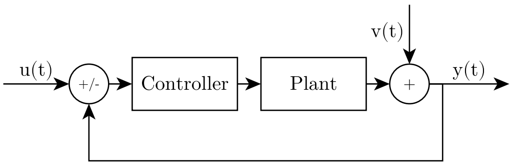

Figure 31: An closed-loop system containing a controller and a plant, with an input, output and disturbance ($u(t), y(t), v(t)$, respectively).

Classical solutions for this problem are: [19, 17, 28]

- Direct identification - “Ignore the feedback and identify the open-loop system using measurements of the input and the output" [15].
- Indirect identification - “Identify some closed-loop transfer function and determine the open-loop parameters using the knowledge of the (linear) controller" [15].
- Joint input/output identification - “Regard the input and output jointly as the output from a system driven by some extra input or set-point signal and noise. Use some method to determine the

> open-loop parameters from an estimate of this augmented system" [15]

The relatively simple direct approach remains popular. In recent literature it appears “that prediction error identification methods [PEM], applied in a direct fashion will provide correct estimates in a number of feedback cases. Furthermore, the accuracy is not necessarily worse in the presence of feedback" [17]. Also, recent methods “can be viewed as special parametrizations of the general prediction error method" [15]. To put it even stronger: *“The optimal statistical properties, the simplicity, and the general applicability of the direct method implies that this should be seen as the first choice of methods for closed-loop identification. When this method fails no other method will succeed"* [15]. Usually, this will result in a high order model, which can be simplified in a later step.

An overview of closed-loop identification methods have been published by Hof and Schrama [20], Gustavsson et al. [17], Hof [19], Forssell [15]. The articles describe newer approaches including the *Instrumental Value, Tailor-made, Coprime factorisation* and *Dual Youla* method. Additionally, Baselli and Bolzern [4] wrote a survey article in biomedical context because “Closed-loop identification is a frequently encountered problem in the biomedical field".

### A.2.2 *Recursive identification*

Another active topic in the system identification area is recursive system identification. Usually, the identification is performed with the entire data set in order to obtain a model. However, when new data becomes available, it is not efficient and probably computational expensive to re-run the identification process, especially when the new data is provided every sampling time step. Recursive system identification focusses on on-line calculation of the model. Chen [7] reviews this recursive method for linear and non-linear parametric models.

### A.2.3 *Soft-computing as identification tool*

Fuzzy logic and artificial neural networks (ANN) can be used as a system identification tool. Both are inspired by biological processes.

#### *Fuzzy logic*

Fuzzy logic can be explained by context related ‘if...then...’ rules and can model partial truth through linguistic expressions [12]. “*We can see that fuzzy implications as well as fuzzy sets are very suitable to describe the process of human thinking*" [47]. Extracting fuzzy rules from a system is currently an active topic in research and can be rather complex. There are several studies about fuzzy rule extraction, and a framework has not been established yet [47] although Mitra and Hayashi [32] proposes one. Fuzzy rule extraction literature is, among many others, written by [52, 22, 2, 8, 38, 48, 37]. They discuss different extraction methods and applications, but roughly all of the methods can be applied to human operator control identification. The difference between the extraction methods is mainly a trade-off between accuracy and complexity of the method.

*Artificial Neural Networks*

Entzinger [12] describes artificial neural networks as: "*(Artificial) Neural networks (NNs) are mathematical constructs for mapping input/output data based on an analogy with the (human) brain. Like the human brain, the NNs consist of several elementary information processing units called 'neurons', which are interconnected by weight functions, the equivalent of synapses in the brain. Typically the neuron output is triggered if the sum of (weighted) synaptical inputs reaches a certain value, generally called 'bias'. The weights and bias values are the main parameters of the neural network model. The proper values for the weights and biases can be trained from sample input/output data*".

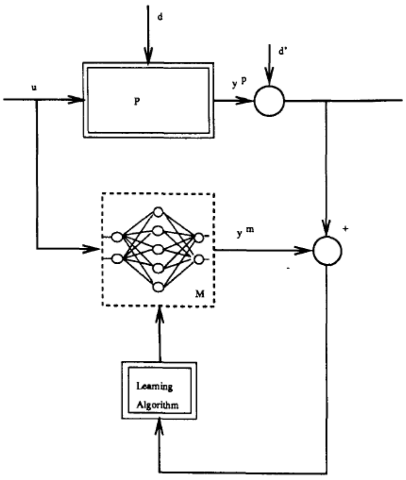

Figure 32: Artificial Neural Network $M$ in an identification setup [23]

Neural networks have the ability to identify linear and non-linear dynamics. This can be done in various ways, where the so-called *forward modelling* method is the most intuitive one. Here, the ANN is trained parallel with the system. The prediction error the ANN makes will be used to adjust the model [23]. See Figure 32. Another way to describe dynamical LTI and LTV systems is by using a Hopfield Neural Model, which is a form of parametric identification [9] that can model system memory. This identification method is less straight-forward than the previously described method. A drawback of using ANN's in identification tasks is that it does not explain the underlying mechanism, it just fits input to output data.

*Neuro-fuzzy models*

The two soft-computing models can also be combined to form a neural-fuzzy architecture. *"Neuro-fuzzy modelling is a flexible framework in* *which different paradigms can be combined, providing, on the one hand, a transparent interface with the designer and, on the other hand, a tool for accurate non-linear modelling and control. The rule-based character of neuro-fuzzy models allows for the analysis and interpretation of the result"* [3].

Typical neuro-fuzzy models are POPFNN (Pseudo Outer-Product-Based Fuzzy Neural Networks) and ANFIS (Adaptive-Network-Based Fuzzy Inference System). They use input-output pairs to model system dynamics, like any identification paradigm. In fact, "[ANFIS] can replace almost any neural networks in control systems to serve the same purposes" [24], but with (for humans) more understandable fuzzy rules. With these systems, one can make a trade-off: interpretability and accuracy of the model.

# B

# VALIDATION OF IDENTIFICATION METHODS

Before analysing to human-in-the-loop situation, the system identification methods have been investigated. Open-loop and closed-loop simulations have been performed *without* the presence of a human controller. Instead, a PID controller replaces the human pilot. This approach allows to bypass the potentially complex human control action. Figure 33 shows the block diagrams of the open- and closed-loop situation.

## B.1 GOAL

The goal of this intermediate experiment is to find out if the PID controller dynamics can be obtained using input and output data.

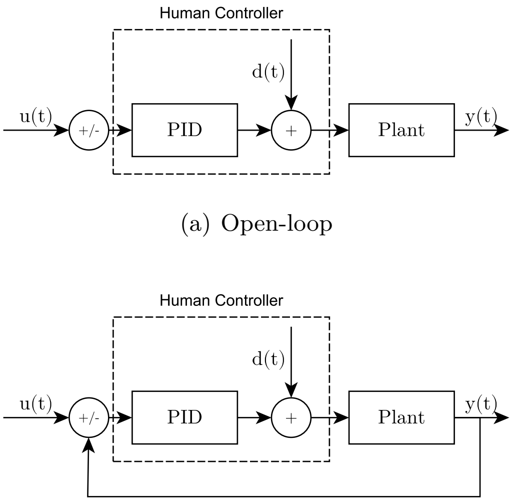

(a) Open-loop

(b) Closed-loop

Figure 33: In order to test closed-loop identification techniques, the human pilot has been replaced by a PID controller. Hence, open-loop and closed-loop simulations can be performed

## B.2 METHODS AND MATERIALS

A discrete PID controller replaces the human pilot. The controller is configured with the `pidtool` MATLAB PID tuning toolbox to have a certain transient response. In the closed-loop, the system should have a rise time of 1 second for 1 degree of pitch change. The controller settings are calculated as:

$$C = k_p + k_i \frac{T_s}{z-1} + k_d \frac{z-1}{T_s} \tag{46}$$

$$k_p = 1.79, \qquad k_i = 2.44, \qquad k_d = 0.171, \qquad T_s = 0.05s \tag{47}$$

The aircraft model is a simple second-order mass-spring-damper system with a cross-over frequency which matches the B747-400 ($\omega_c \approx 0.5$Hz, $m = 260 \cdot 10^3$ kg B747-400 maximum landing weight, $d = 1 \cdot 10^6$ in order to have slightly damped poles, and $k = 4m$ N/m, for $w_n = 2$rad/s).

$$P(s) = \frac{k}{ms^2 + ds + k} \rightarrow \tag{48}$$

$$P(z) = \frac{0.00469z + 0.004399}{z^2 - 1.816z + 0.8251} \tag{49}$$

$$\tag{50}$$

The PRBS input signal is the same as in Chapter 3 and switches the FD between -3 and 3 degrees pitch. The noise input $d(t)$ simulates the human inherent control noise and is Gaussian white noise with $\sigma_d^2 = 1$ degrees pitch (which is rather high compared to the signal-to-noise ratio as suggested in Chapter 3).

## B.3 ANALYSIS OF RESULTS AND CONCLUSION

The PID controller and aircraft model can be loaded to SIMULINK and the output can be simulated in real-time. The input and output data are saved for the identification of the PID controller.

### B.3.1 *Pre-processing*

Before any identification method, it is required to split the experiment data into a identification and validation data-set. Hence, these will be de-trended and removed of its means. As the PRBS is within the human bandwidth, it already has the emphasis on low-frequency content. Low-pass pre-filtering the data, with for instance a Butterworth filter, is not necessary.

### B.3.2 *Model structure*

Linear parametric model-sets will be used for the system identification process. In this report, the common ARX will be used, as well as the OE model-set (see Appendix A). This is because the simulation involves the addition of Gaussian white noise. OE models are particularity well in fitting systems perturbed by white noise as can be seen by the following equations. The ARX model:

$$A(z)y(t) = B(z)u(t) + v(t) \tag{51}$$

$$y(t) = \frac{B(z)}{A(z)}u(t) + \frac{1}{A(z)}v(t) \tag{52}$$

and the OE model:

$$y(t) = \frac{B(z)}{F(z)}u(t) + v(t) \tag{53}$$

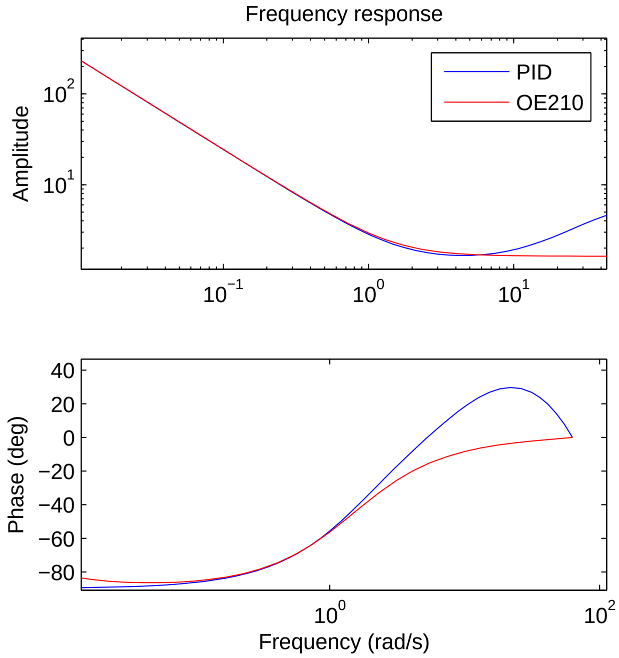

Figure 34: The frequency response of the open-loop PID controller versus OE210 model predictions. Within the frequency range of the PRBS input signal, the model estimates the PID controller accurately.

### B.3.3 *Open-loop*

For the open-loop experiment, a OE210 fits has an excellent model fit (over 90%) and from the residual tests it can be deducted that the model residuals are uncorrelated (see Chapter 3 for the procedure of these tests). The frequency response of the actual PID controller is compared to the OE210 model predictions in Figure 34. Especially in the low-frequency range the model performs well. There is some discrepancy at in the high-frequency range. That can be explained by the fact that the input signal mainly doesn't contain such high-frequent excitations. Identification will therefore be difficult in that frequency scope.

### B.3.4 *Closed-loop*

As discussed in Chapter 3 and Appendix A, closed-loop identification can be challenging due to correlated input, noise and output channels.

First of all, the closed-loop (system input to system output) can be modelled sufficiently well with an ARX331 model. The model has a 92% fit and model residuals are uncorrelated with the input and with itself.

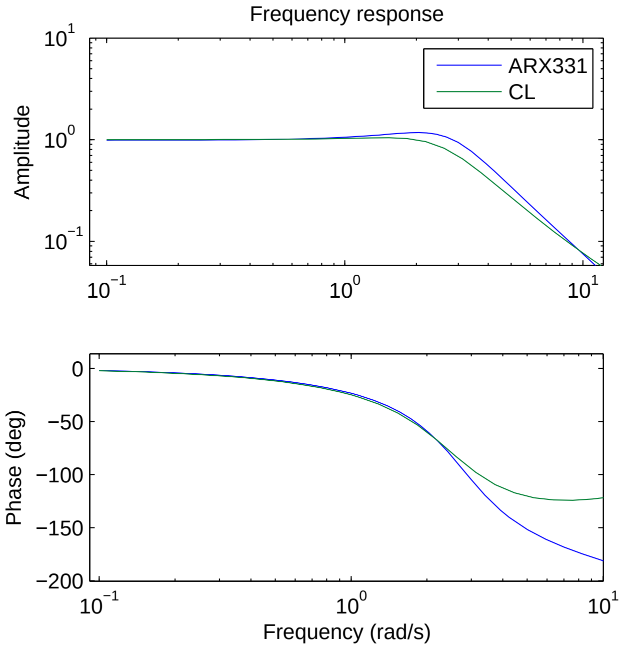

Figure 35: Closed-loop frequency response versus the ARX331 predictions

The frequency response can be observed in Figure 35 and the impulse response in Figure 36. Again, within the frequency range of the PRBS input signal, the model estimates the closed-loop rather well.

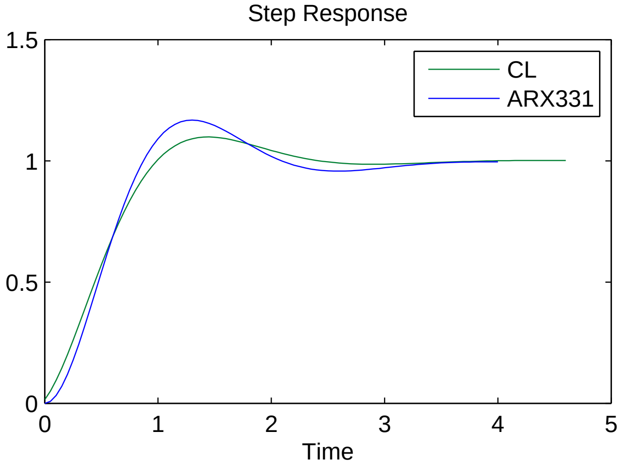

Figure 36: Closed-loop impulse response of the simulated system versus the ARX331 prediction

The direct closed-loop identification approach is used to find the controller dynamics. In Figure 37, the OE210 reveals a similar frequency response to the actual simulated PID controller, however with a certain bias over the whole frequency range. The model fit of the OE210 is less than the open-loop situation and the model residuals are not uncorrelated with the input. Still, the predictions do mimic the PID controller's response.

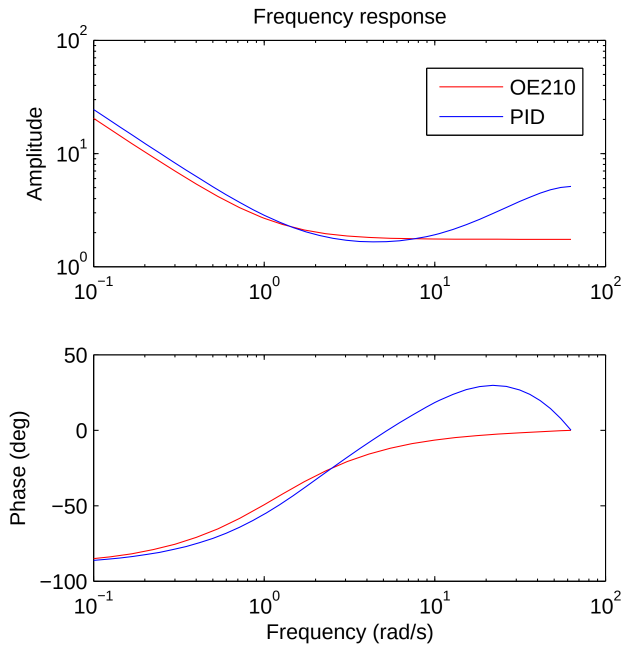

Figure 37: The frequency response of the closed-loop PID controller versus OE210 model predictions. Within the frequency range of the PRBS input signal, the model estimates the PID controller, with a bias.

It can be concluded that the PID controller can be identified in the closed-loop, but the solution do not yield unbiased models over the whole frequency scope. The closed-loop residuals are still correlated with the input, and therefore are not as consistent as in an open-loop situation.

## B.4 DISCUSSION

Although the PID controller was estimated in the closed-loop, it doesn't guarantee that this approach will work for other systems. Especially if the controller and plant dynamics are increasingly complex, system identification often requires a tailored approach [28]. Other closed-loop methods as discussed in Appendix A could provide more accurate results. However, only the direct identification approach has been evaluated.

C

# INVESTIGATING FLIGHT SIMULATOR LONGITUDINAL DYNAMICS

For simulation purposes, a model of aircraft dynamics is essential. For this report, especially aircraft motion in the pitch direction is useful to investigate. In Chapter 3, three experiments have been outlined. For the computer simulation experiment, longitudinal dynamics of the aircraft are used in the closed-loop system. Within the experiment setup, it is relatively easy to load various models. On the other hand, the University of Tokyo has a fixed-base B747-400 flight simulator. It turns out to be complicated to port the experiment to the flight simulator computer[1]. Therefore, it chosen to capture the simulator's longitudinal dynamics and transfer these to the computer with experiment setup (using MATLAB and SIMULINK ).

## C.1 GOAL

For the investigation of the B747-400 simulated pitch dynamics, an identification experiment is designed. It uses elevator input and pitch output data to construct a parametric model. The objective of the experiment is to obtain a model that is usable for aircraft simulation.

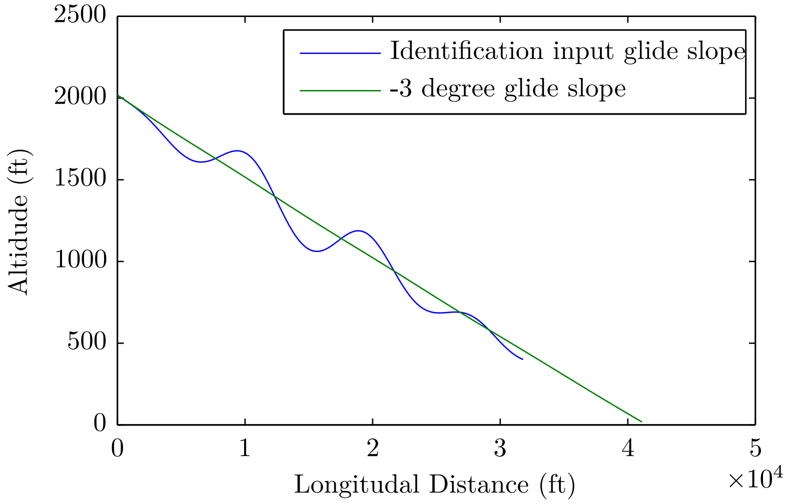

Figure 38: The glide slope of the B747 during the identification experiment

[1] Apparently, it was hard to manipulate the FD on the Attitude Indicator of the simulator. The simulator from the University of Tokyo runs two separate simulation engines, from which only one can be fully customized. Probably, it would be possible to port the experiment setup, but that would involve a substantial amount of coding.

## C.2 METHODS AND MATERIALS

The experiment is based on techniques from frequency system identification. An input signal would override the elevator input normally controlled by the pilot through the yoke. Note that the aircraft is now identified in an open-loop system which makes it possible to use well-established open-loop identification techniques. Optimally, the input signal would be a sort of random signal, but it was more convenient to use a sine-wave signal[2]. Several experiments have been conducted, each with a sine-wave with different amplitude and frequency (see Table 4).

| Frequency [Hz] | Elevator input amplitude [degrees] |
|---|---|
| 0.0316 | 0.02 |
| 0.0599 | 0.02 |
| 0.1136 | 0.1 |
| 0.2154 | 0.1 |
| 0.4084 | 0.1 |

Table 4: Frequency and amplitude of the sine-wave for frequency identification of the B747-400 longitudinal dynamics

The B747-400 flight simulator is set to approach settings: flaps 30 degrees, speed 180 knots, but with landing gear up. The glide-slope is set to -3 degrees, as can be seen in Figure 38.

Hence, the pitch response of the aircraft is recorded and compared with the elevator input resulting in a amplitude and phase difference for each tested frequency. These data points can be shown in a Bode plot as in Figure 39. Using the Sanathanan and Koerner [41]-algorithm from the MATLAB freq-id toolbox [10], a transfer function has been generated to fit the data points in frequency domain. The continuous transfer function is shown as the green line in Figure 39.

## C.3 ANALYSIS OF RESULTS AND CONCLUSION

The transfer function has the form of a second-order system, illustrating the aircraft as a mass-spring-damper system:

$$P(s) = \frac{0.102}{s^2 + 0.1201s + 0.001295} \tag{54}$$

When this frequency response is observed thoroughly, one can find a low-frequent pole beyond the lowest measurement frequency. This pole could be placed even more to the low-frequent resulting in a pure integrator (i,e. $\frac{1}{s}$ in Laplace-domain). The aircraft can now be modelled as a mass-damper system with low-frequent integrating action and the

[2] In order to override the elevator input, some changes needed to be made to the Flight Simulator code. A sine-wave was implemented easier than a random signal

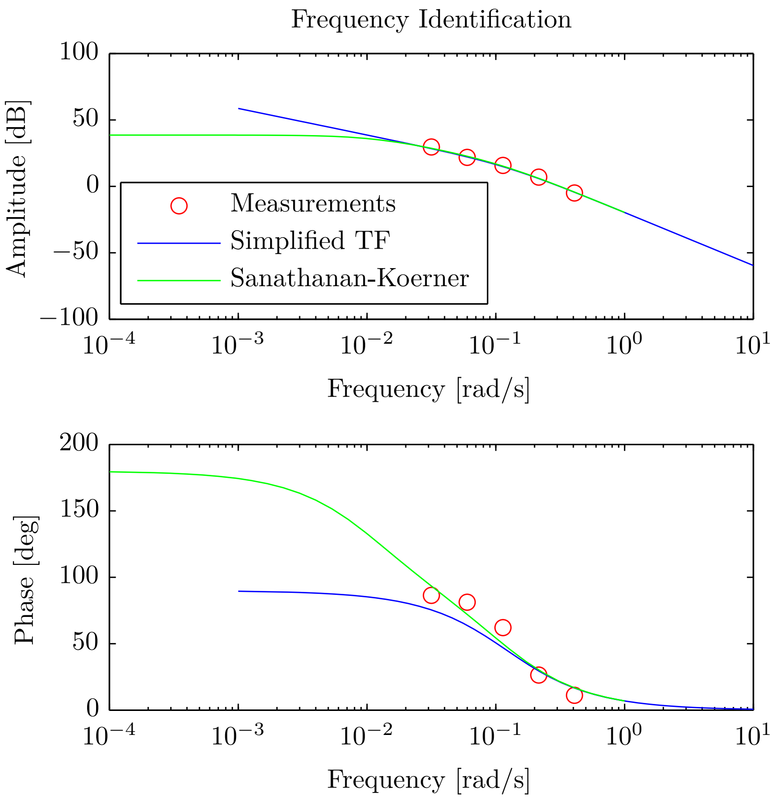

Figure 39: A second-order mass-spring-damper model and its mass-damper simplification. The measurement data is shown as red dots

transfer function fits the measurements approximately as well as the second-order model.

$$P(s) \approx \frac{1}{s}\frac{0.102}{s+0.1201} \tag{55}$$

The obtained continuous transfer function is suitable for aircraft simulation and can be implemented in the computer simulation experiment from Chapter 3.

## C.4 DISCUSSION

Although the obtained transfer function is continuous and defined for the entire frequency band, it is based on only a few measurements. Only the mid-frequency range is actually based on the B747-400 flight simulator dynamics, the low- and high-frequency scope are ‘extrapolated’. The real flight simulator dynamics might show significant discrepancies in those regions. This is noticed by the human pilot during simulations and preliminary tests of this model.

Extending the measurements with more low-frequent and high-frequent input sine-waves does not work due to the long simulation time, insufficient integration accuracy of the flight simulator for high-frequency inputs and excitation of low-frequent aircraft modes such as the *fugoid*.

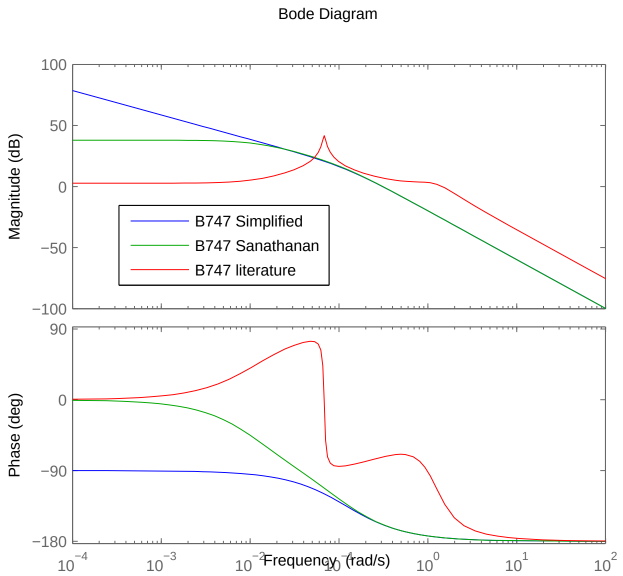

Figure 40: Comparison of the aircraft models

The model is compared to the B747-400 longitudinal dynamics from [25] in Figure 40. As can be seen, the identified model only captures a part of the characteristics. The shift over the frequency axis is possibly due to different initial conditions of the aircraft (the flight simulator is set to approach settings, whereas the [25]'s model is based on cruising speed).

A reason that the identified B747-400 model is hard to control is that the low-frequent integrating character of the aircraft will increase the control error rapidly. The pilot can avoid this by controlling at a higher frequency, passing the integrating action. This phenomenon is discussed in Chapter 6.

For the computer simulation experiment, the model of the flight simulator longitudinal dynamics is not used due to the issues described above. Instead, the model from [25] is loaded to the simulation. It might be possible to derive the pitch dynamics directly from the aircraft's equations of motion. However, this report does not cover further investigation of the flight simulator dynamics.

# D INVESTIGATING REACTION TIME DELAY

Feedback channels are provided to the human pilot to base his control action upon. Experiments as described in Chapter 3 rely on visual feedback of the FD on the attitude indicator. It is known that human subjects have a reaction time delay, i.e. the time difference between the provided input signal and corresponding control action. Through a sequence of experiments, the lag due to reaction time of the different human subjects is investigated.

## D.1 GOAL

The objective of the experiment is to gain insight in the delay of the pilot's response. This could provide valuable information for modelling human pilot pitch control in Chapter 4.

## D.2 METHODS AND MATERIALS

In order to find the *minimum* reaction time delay, a simple experiment is designed using a keyboard and a computer with MATLAB installed. A black window is shown to computer screen. Each subject is asked to press any button on the keyboard, as quickly as possible when the window turns from black to white. This is done 10 times with a random interval (any value between 1 and 5 seconds) between the black and white window. The reaction time delay is recorded and saved to a file. Every subject performs this experiment three times, so 30 data points per pilot are obtained.

## D.3 ANALYSIS OF RESULTS AND CONCLUSION

After processing the data, the reaction time delays of the subjects seemed to be log-normally distributed. This could be verified by plotting a histogram with $n$-bins[1] and looking at the 'convex hull' of the figure. Its shape did not resemble a probability density function of a normal distribution, but rather a log-normal distribution, which is supported by literature [49].

Figure 41 shows the results for 5 tested subjects: 2 student non-pilot subjects (STI, STL), 2 non-pilot researchers (REA, REB) and 1 retired B747 captain (CPT). Note that the x-axis is the logarithm of the reaction time delay. When the data is combined by assuming all data is from a 'single average pilot', plotting the log-normal distribution

[1] The value of $n$ is found iteratively, until the shape of the probability density function can be distinguished

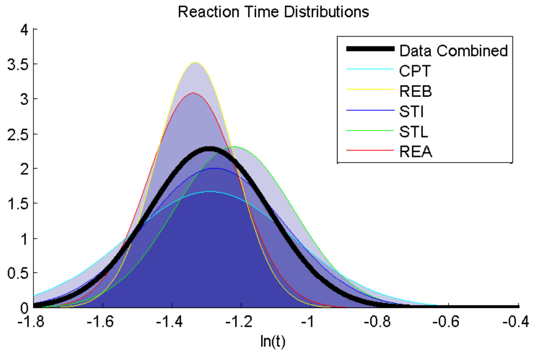

Figure 41: Log-normal distributed reaction time delays for 5 tested subjects. The expected time delay can be found as the peak of the combined data: 0.28 seconds

results in the light grey area. The average reaction time delay to expect in the data therefore is $e^{-1.29} = 0.28$ seconds.

## D.4 DISCUSSION

This experiment will give an indication of the minimum reaction time delay because this setup enables the pilot to give direct feedback when the window turns white. The window is the pilot's centre of attention. In aircraft control, the switching of FD commands possibly is not directly recognized by the pilot because there are many other indicators to focus on and thus will increase the reaction time. Other experiments could be made to investigate this 'scanning' phenomenon, but for the scope of this report, an indication of the minimum reaction time delay is sufficient.

Furthermore, a remark has to be made concerning the combination of the data to obtain the average lag. It might not be statistically correct to create a 'single average pilot' in this manner. Some pilots might systematically have a lower or higher delay and might need to be treated differently when the pilot pitch control models are created. In Chapter 4, however, the reaction time delay obtained from this experiment is only used as a guideline and the order of magnitude of what can be expected to be the delay in the data.

# E

# EXPERIMENT SOFT/HARDWARE SETUP

The experiments from Chapter 2 are described using the block diagram in Figure 42 and Table 5.

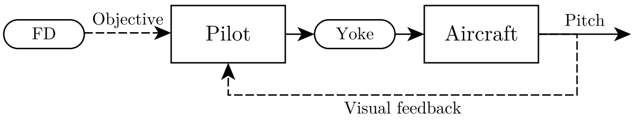

Figure 42: The experiment setup

| | Testing identification techniques | Computer simulation | Flight simulator |
|---|---|---|---|
| FD signal | PRBS | PRBS | PRBS |
| Pilot | PID controller | 1 retired airline B747 captain, 3 trained non-pilot subjects | 1 retired airline B747 captain, 1 trained non-pilot subject |
| Yoke | Logitech Joystick Extreme 3D Pro | The University of Tokyo, Suzuki-Tsuchiya lab sim yoke | Flight simulator's yoke |
| Aircraft model | Second order system (Appendix B) | B747-400 longitudinal dynamics [25], Appendix C | JAXA's Dornier Do-228-200 full flight simulator |
| Others | Intel Core 2 Duo CPU, 2.80 GHz, 4 GB RAM, Windows 7 64-bit. MATLAB R2013a, Simulink AI | | Flight simulator processors and instruments |

Table 5: Software and hardware specifications for the experiments conducted during the internship

# PILOT IDENTIFICATION TOOLBOX

For the experiments and analyses in this report, several MATLAB and Simulink scripts have been written. The source codes have been combined into one toolbox: the `Pilot Identification Toolbox/`. The essential files will be highlighted in this Appendix.

## F.1 ACQUIRING EXPERIMENT DATA

Within the folder `Experiments/`, the tools to acquire experiment data are presented.

| Source file | Description |
|---|---|
| `Target Input Generation/` | Folder containing tools to generate the PRBS and multi-sine FD inputs. |
| `inputGenerator.m` | Script to generate tab-separated ([time,pitch]) input files for the experiments. Outputs a PRBS and a multi-sine file. |
| `signalCheck.m` | Script to analyse a signal's PSD (Periodogram, Welch), RMS, Crest value, PE-order and computes a bandwidth approximation |
| `PID/` | Folder containing tools to collect and process simulation data for the PID experiment. |
| `PID_OL_getdata.m` | MATLAB script to run the open-loop PID experiment simulation. |
| `PID_CL_getdata.m` | MATLAB script to run the closed-loop PID experiment simulation. |
| `PID_OL_id.m` | MATLAB script to prepare the open-loop PID experiment simulation data for processing in `ident`. |
| `PID_CL_id.m` | MATLAB script to prepare the closed-loop PID experiment simulation data for processing in `ident`. |
| `Aircraft.m` | Simulated second order aircraft model. |
| `PID_CL_sim.slx`,<br>`PID_CL_sim_noFD.slx`,<br>`PID_OL_sim.slx`,<br>`PID_OL_sim_noFD.slx` | Simulink models for simulation with and without FD output. |

| | |
|---|---|
| `PID/IdentSessions/` | Folder containing saved `ident` sessions for processing the PID experiment data |
| `JAXA/FDoverride/` | Folder containing scripts to generate text files that override the JAXA FD indicator on the simulator's AI. |
| `readFD.m`, `writeFD.m` | MATLAB scripts to read and write the text files that override the FD |
| `HIL/Joystick`,<br>`HIL/Yoke` | Folder containing tools to set up a computer simulation as described in this report. This can be done with a computer and a joystick, or a computer and a flight simulator yoke, respectively. |
| `/Joystick/`<br>`systemxFD_getdata.m` | Script that performs real-time simulation. Calls `systemxFD_sim.slx`, an input signal and aircraft model. |
| `/Yoke/`<br>`FSimxFD_getdata.m` | Script that performs real-time simulation. Calls `FSimxFD_sim.slx`, an input signal and aircraft model. |
| `/Joystick/`<br>`systemxFD_id.m` | Script that prepares the data acquired by the `_getdata` for later processing with tools from the Pilot modelling folder. |
| `/Yoke/ FSimxFD_id.m` | Script that prepares the data acquired by the `_getdata` for later processing with tools from the Pilot modelling folder. |
| `HIL/../Instruments/` | Folder containing the graphics for the AI and FD in SIMULINK . Note that the path of these graphics might need manual adjustment in the `.slx` files. |

Table 6: Explanation of the tools in the Experiment folder

## F.2 PILOT MODELLING

| Source file | Description |
|---|---|
| `JAXA/` | This report only covers the analysis of the full flight simulator data (obtained with the JAXA simulator). The tools in this folder can, however, also be used for the analysis of other experiments. |
| `/ExperimentSet1`,<br>`/ExperimentSet2` | Folder containing the raw flight simulator data. Ordered in sub-folders |

| | |
|---|---|
| `readJAXA.m` | Reads the raw data and outputs an array of the data channels that need to be processed. The array is filled with [pitch 1, elevator 1, FD 1, pitch 2, elevator 2, FD 2], where 1 is the identification dataset and 2 is the validation dataset. |
| `plotJAXA.m` | Plots the pitch, elevator deflection and FD signal with respect to time in a single figure. |
| `ARX_CL.m` | MATLAB script to analyse the closed-loop behaviour through linear parametric models. Needs manual processing with `ident` by importing the `iddata` variables in the GUI. The results are saved as `CL_models.mat`. |
| `ARX_JAXA.m` | MATLAB script to analyse the controller dynamics through a linear parametric ARX model. It automatically estimates a suitable model order or a manual `ident` controller can be loaded to the script. Outputs training and validation results, system's response, prediction accuracy and calculation time. |
| `NN_JAXA.m` | MATLAB script to analyse the controller dynamics with a NN. Uses the Neural Network Toolbox. Network properties can be adjusted by changing parameters in the script. Outputs training, validation and testing results, system's response, prediction accuracy and calculation time. |
| `ANFIS_JAXA.m` | MATLAB script to analyse the controller dynamics with ANFIS. Uses the Fuzzy Logic Toolbox. Inference system properties can be adjusted by changing parameters in the script. Outputs training and validation results, system's response, prediction accuracy and calculation time. |

Table 7: Explanation of the tools in the Pilot Modelling folder

## F.3 OTHERS

| Source file | Description |
|---|---|
| `ARMASA/` | Toolbox for spectral density estimation. The toolbox is used for residual analysis as shown in Chapter 4. |

| | |
|---|---|
| `Interactive Aircrafts/` | Tools to simulate different aircraft dynamics in real-time. Can be used to illustrate the change of aircraft 'feel' interactively by changing the aircraft model. |
| `Reaction Time/` | Tools for determining the minimum expected reaction time delay. See Appendix D. |
| `UTSim Identification/` | Tools for determining the longitudinal dynamics of the University of Tokyo flight simulator through frequency identification techniques. See Appendix C. |

Table 8: Other tools in the Pilot Identification Toolbox

# BIBLIOGRAPHY

[1] Ronald Aarts. System Identification and Parameter Estimation. *University of Twente, Faculty of Engineering Technology*, 2012.

[2] Robert Andrews, Joachim Diederich, and Alan B. Tickle. Survey and critique of techniques for extracting rules from trained artificial neural networks. *Knowledge-Based Systems*, 8(6):373–389, December 1995. ISSN 09507051. doi: 10.1016/0950-7051(96)81920-4. URL http://linkinghub.elsevier.com/retrieve/pii/0950705196819204.

[3] Robert Babuška and Henk Verbruggen. Neuro-fuzzy methods for nonlinear system identification. *Annual Reviews in Control*, 27(1):73–85, January 2003. ISSN 13675788. doi: 10.1016/S1367-5788(03)00009-9. URL http://linkinghub.elsevier.com/retrieve/pii/S1367578803000099.

[4] G Baselli and P Bolzern. Closed-Loop System Identification. *Wiley Encyclopedia of Biomedical Engineering*, 2006. URL http://onlinelibrary.wiley.com/doi/10.1002/9780471740360.ebs0279/full.

[5] PMT Broersen. Automatic spectral analysis with time series models. *Instrumentation and Measurement, IEEE . . .* , 51(2):211–216, 2002. URL http://ieeexplore.ieee.org/xpls/abs_all.jsp?arnumber=997814.

[6] Ozkan Celik and Seniz Ertugrul. Predictive human operator model to be utilized as a controller using linear, neuro-fuzzy and fuzzy-ARX modeling techniques. *Engineering Applications of Artificial Intelligence*, 23(4):595–603, June 2010. ISSN 09521976. doi: 10.1016/j.engappai.2009.08.007. URL http://linkinghub.elsevier.com/retrieve/pii/S0952197609001341.

[7] Han-Fu Chen. Recursive system identification. *Acta Mathematica Scientia*, 29(3):650–672, May 2009. ISSN 02529602. doi: 10.1016/S0252-9602(09)60062-X. URL http://linkinghub.elsevier.com/retrieve/pii/S025296020960062X.

[8] S Chiu. Extracting fuzzy rules from data for function approximation and pattern classification. *Fuzzy Information Engineering: A Guided Tour of . . .* , pages 1–10, 1997. URL http://chius.homestead.com/files/ExtractRulesFromData.pdf.

[9] SR Chu, Rahmat Shoureshi, and Manoel Tenorio. Neural networks for system identification. *Control Systems Magazine, . . .* , (April):31–35, 1990. URL http://ieeexplore.ieee.org/xpls/abs_all.jsp?arnumber=55121.

[10] R A de Callafon. FREQID, a GUI for frequency domain identification. pages 1–31, 2000.

[11] J. O. Entzinger and T. Uemura. Mental effort and safety in curved approaches. pages 1–11.

[12] J.O. Entzinger. *Analysis of Visual Cues for Human Pilot Control in the Final Approach and Landing.* PhD thesis, University of Tokyo, 2010.

[13] J.O. Entzinger, M. Nijenhuis, T. Uemura, and S. Suzuki. Assessment of human pilot mental workload in curved approaches. *Asia-Pacific International Symposium on Aerospace Technology (APISAT 2013)*, pages 2–7, 2013. URL http://doc.utwente.nl/89814/.

[14] Seniz Ertugrul. Predictive modeling of human operators using parametric and neuro-fuzzy models by means of computer-based identification experiment. *Engineering Applications of Artificial Intelligence*, 21(2):259–268, March 2008. ISSN 09521976. doi: 10.1016/j.engappai.2007.03.007. URL http://linkinghub.elsevier.com/retrieve/pii/S0952197607000474.

[15] Urban Forssell. Closed-loop identification: Methods, theory, and applications. (566), 1999. URL http://www.diva-portal.org/smash/record.jsf?pid=diva2:652232.

[16] Aditya Chandrashekhar Gondhalekar. *Strategies for non-linear system identification.* PhD thesis, Imperial College London, 2009.

[17] I Gustavsson, Lennart Ljung, and Torsten Soderstrom. Survey Paper Identification of Processes in Closed Loop. Technical report, 1977.

[18] Y. Hashambhoy and R. Vidal. Recursive Identification of Switched ARX Models with Unknown Number of Models and Unknown Orders. *Proceedings of the 44th IEEE Conference on Decision and Control*, pages 6115–6121, 2005. doi: 10.1109/CDC.2005.1583140. URL http://ieeexplore.ieee.org/lpdocs/epic03/wrapper.htm?arnumber=1583140.

[19] Paul Van Den Hof. Closed-loop issues in system identification. *Annual reviews in control*, 22:173–186, 1998. URL http://www.sciencedirect.com/science/article/pii/S1367578898000169.

[20] P.M.J. Van Den Hof and R.J.P. Schrama. Identification and control-closed-loop issues. *Automatica*, 31(12):1751–1770, 1995. URL http://www.sciencedirect.com/science/article/pii/000510989500094X.

[21] Kurt Hornik. Approximation capabilities of multilayer feedforward networks. *Neural networks*, 4(1989):251–257, 1991.

URL http://www.sciencedirect.com/science/article/pii/089360809190009T.

[22] Chongfu Huang and Claudio Moraga. Extracting fuzzy if-then rules by using the information matrix technique. *Journal of Computer and System Sciences*, 70(1):26–52, February 2005. ISSN 00220000. doi: 10.1016/j.jcss.2004.05.001. URL http://linkinghub.elsevier.com/retrieve/pii/S0022000004000650.

[23] KJ Hunt, D Sbarbaro, R Zbikowski, and PJ Gawthrop. Neural networks for control systemsâĂŤa survey. *Automatica*, 28(6):1083–1112, 1992. URL http://www.sciencedirect.com/science/article/pii/000510989290053I.

[24] JSR Jang. ANFIS: adaptive-network-based fuzzy inference system. *Systems, Man and Cybernetics, IEEE Transactions . . .*, 23(3), 1993. URL http://ieeexplore.ieee.org/xpls/abs_all.jsp?arnumber=256541.

[25] K Kosar, S Durmaz, and EM Jafarov. Longitudinal dynamics analysis of Boeing 747-400. *Proceedings of the 9th WSEAS . . .*, pages 82–87, 2007. URL http://dl.acm.org/citation.cfm?id=1973552.

[26] H Kwakernaak and G Meinsma. Time Series Analysis and System Identification. *University of Twente, Department of Applied Mathematics*, 2013.

[27] VA Laurense, DM Pool, and HJ Damveld. Effects of Controlled Element Dynamics on Human Feedforward Behavior in Ramp-Tracking Tasks. *ieeexplore.ieee.org*, pages 1–13, 2014. URL http://ieeexplore.ieee.org/xpls/abs_all.jsp?arnumber=6824242.

[28] Lennart Ljung. *System identification-Theory for the user, second edition*. Prentice Hall PTR, Linköping University, Sweden, May 1999. ISBN 0136566952.

[29] Lennart Ljung. Perspectives on system identification. *Annual Reviews in Control*, 34(1):1–12, April 2010. ISSN 13675788. doi: 10.1016/j.arcontrol.2009.12.001. URL http://linkinghub.elsevier.com/retrieve/pii/S1367578810000027.

[30] DT McRuer. Human pilot dynamics in compensatory systems. 1965. URL http://oai.dtic.mil/oai/oai?verb=getRecord&metadataPrefix=html&identifier=AD0470337.

[31] DT McRuer and ES Krendel. Mathematical models of human pilot behavior. (January), 1974. URL http://oai.dtic.mil/oai/oai?verb=getRecord&metadataPrefix=html&identifier=AD0775905.

[32] Sushmita Mitra and Yoichi Hayashi. Neuro-fuzzy rule generation: survey in soft computing framework. *Neural Networks, IEEE*

*Transactions on*, 11(3):748–768, 2000. URL http://ieeexplore.ieee.org/xpls/abs_all.jsp?arnumber=846746.

[33] MC Nechyba and Yangsheng Xu. Human control strategy: abstraction, verification, and replication. *Control Systems, IEEE*, 1997. URL http://ieeexplore.ieee.org/xpls/abs_all.jsp?arnumber=621469.

[34] Marijn Nijenhuis. Master Internship Report - Measuring pilot-affected safety of flight. *University of Twente*, 2013.

[35] Marijn Nijenhuis. Pilot modelling, literature review (Unpublished). Technical report, University of Twente, 2013.

[36] P Van Overschee and B De Moor. N4SID: Subspace algorithms for the identification of combined deterministic-stochastic systems. *Automatica*, 311(I):75–93, 1994. URL http://www.sciencedirect.com/science/article/pii/0005109894902305.

[37] M Pasquier, C Quek, and M Toh. Fuzzylot: a novel self-organising fuzzy-neural rule-based pilot system for automated vehicles. *Neural networks : the official journal of the International Neural Network Society*, 14(8):1099–112, October 2001. ISSN 0893-6080. URL http://www.ncbi.nlm.nih.gov/pubmed/11681754.

[38] Nikos Pelekis and B Theodoulikis. Fuzzy miner: extracting fuzzy rules from numerical patterns. *...and Mining (IJDWM)*, pages 1–25, 2005. URL http://www.igi-global.com/article/...extracting-fuzzy-rules/1748.

[39] AV Phatak and GA Bekey. Model of the adaptive behavior of the human operator in response to a sudden change in the control situation. *Man-Machine Systems, IEEE ...*, MM(3):72–80, 1969. URL http://ieeexplore.ieee.org/xpls/abs_all.jsp?arnumber=4081873.

[40] D. M. Pool, P. M. T. Zaal, H. J. Damveld, M. M. Van Paassen, J. C. Van Der Vaart, and M. Mulder. Modeling Wide-Frequency-Range Pilot Equalization for Control of Aircraft Pitch Dynamics. *Journal of Guidance, Control, and Dynamics*, 34(5):1529–1542, September 2011. ISSN 0731-5090. doi: 10.2514/1.53315. URL http://arc.aiaa.org/doi/abs/10.2514/1.53315.

[41] CK Sanathanan and J Koerner. Transfer function synthesis as a ratio of two complex polynomials. *Automatic Control, IEEE ...*, (2):56–58, 1963. URL http://ieeexplore.ieee.org/xpls/abs_all.jsp?arnumber=1105517.

[42] M Schroeder. Synthesis of low-peak-factor signals and binary sequences with low autocorrelation (corresp.). *Information Theory, IEEE Transactions on*, (6), 1970. URL http://ieeexplore.ieee.org/xpls/abs_all.jsp?arnumber=1054411.

[43] JW Senders. The human operator as a monitor and controller of multidegree of freedom systems. *Human Factors in Electronics, IEEE Transactions . . .* , pages 2–5, 1964. URL http://ieeexplore.ieee.org/xpls/abs_all.jsp?arnumber=1698171.

[44] Galit Shmueli. To Explain or to Predict? *Statistical Science*, 25(3): 289–310, August 2010. ISSN 0883-4237. doi: 10.1214/10-STS330. URL http://projecteuclid.org/euclid.ss/1294167961.

[45] Torsten Söderström and Petre Stoica. *System identification*. Prentice Hall PTR, Uppsala, Bucharest, 1989. ISBN 0-13-881236-5.

[46] P Stoica and RL Moses. *Spectral analysis of signals*. Prentice Hall PTR, 2005. ISBN 0131139568. URL http://user.it.uu.se/~ps/SAS-new.pdf.

[47] M Sugeno and M Nishida. Fuzzy control of model car. *Fuzzy sets and systems*, 16:103–113, 1985. URL http://www.sciencedirect.com/science/article/pii/S0165011485800117.

[48] Tomohiro Takagi and Michio Sugeno. Fuzzy identification of systems and its applications to modeling and control. *IEEE Transactions on Systems, Man, and Cybernetics*, SMC-15(1):116–132, January 1985. ISSN 0018-9472. doi: 10.1109/TSMC.1985.6313399. URL http://ieeexplore.ieee.org/lpdocs/epic03/wrapper.htm?arnumber=6313399.

[49] R Ulrich and J Miller. Information processing models generating lognormally distributed reaction times. *Journal of Mathematical Psychology*, 1993. URL http://www.sciencedirect.com/science/article/pii/S0022249683710321.

[50] M Viberg. Subspace-based methods for the identification of linear time-invariant systems. *Automatica*, 31(12), 1995. URL http://www.sciencedirect.com/science/article/pii/0005109895001075.

[51] R Vidal. Identification of spatial-temporal switched ARX systems. *Decision and Control, 2007 46th IEEE Conference on*, pages 4675–4680, 2007. URL http://ieeexplore.ieee.org/xpls/abs_all.jsp?arnumber=4434172.

[52] Liang Wang and John Yen. Extracting fuzzy rules for system modeling using a hybrid of genetic algorithms and Kalman filter. *Fuzzy Sets and Systems*, 101(3):353–362, February 1999. ISSN 01650114. doi: 10.1016/S0165-0114(97)00098-5. URL http://linkinghub.elsevier.com/retrieve/pii/S0165011497000985.

[53] Xing-Song Wang, Chun-Yi Su, and Henry Hong. Robust adaptive control of a class of nonlinear systems with unknown deadzone. *Automatica*, 40(3):407–413, March 2004. ISSN 00051098. doi: 10.1016/j.automatica.2003.10.021. URL http://linkinghub.elsevier.com/retrieve/pii/S000510980300342X.

[54] HT Yang and CM Huang. A new short-term load forecasting approach using self-organizing fuzzy ARMAX models. *Power Systems, IEEE Transactions on*, 13(1), 1998. URL http://ieeexplore.ieee.org/xpls/abs_all.jsp?arnumber=651639.

[55] Deniz Yilmaz, Michael Jump, Lu Linghai, and Michael Jones. State-of-the-art pilot model for RPC prediction report. 2011.